Synthetic Mullite Precursors:
Preparation, Structure, and Transformation Behaviour

Habilitationsschrift zur Erlangung der Lehrbefugnis für das Fachgebiet

Materialwissenschaften

an der

Gemeinsamen Fakultät für Bergbau, Hüttenwesen und Maschinenwesen

der

Technischen Universität Clausthal

vorgelegt von:

Martin Schmücker

Deutsches Zentrum für Luft- und Raumfahrt (DLR)

Institut für Werkstoff-Forschung

51147 Köln

2003

Vorwort

Die vorliegende Habilitationsschrift

"*Synthetic Mullite Precursors: Preparation, Structure, and Transformation Behaviour*"

basiert auf meinen Arbeitsschwerpunkten "*Struktur nichtkristalliner Aluminiumsilikate"* und "*Frühstadien der Mullitbildung"*. Diese Themenbereiche habe ich -neben verschiedenen anderen Aktivitäten- während meiner 10-jährigen Tätigkeit im Institut für Werkstoff-Forschung des DLR konzeptionell entwickelt und kontinuierlich bearbeitet. Die Untersuchungen zur *Struktur nichtkristalliner Aluminiumsilikate* erfolgten zusammen mit internationalen Kooperationspartnern sowie im Rahmen des DFG-Sonderforschungsbereichs 408 (Anorganische Festkörper ohne Translationssysmmetrie, Univ. Bonn). Während diese Arbeiten überwiegend grundlagenorientiert waren, war der Hintergrund für meine Untersuchungen zur *Mullitbildung* stärker anwendungsbezogen: Der Einsatz von mullitbasierter Hochleistungskeramik z. B. für thermisch exponierte Bauteile im Bereich von Luftfahrt, Raumfahrt und Antriebstechnik setzt ein tieferes Verständnis der Mullitbildungsmechanismen voraus.

Es zeigte sich, daß die Arbeiten zur *Mullitbildung* und zur *Struktur der nichtkristallinen Stoffe im System SiO_2-Al_2O_3* eng miteinander verflochten sind. Dabei ergaben sich folgende Kernaussagen:

- Zwischen Mullit und <u>*nichtkristallinen Aluminiumsilikaten*</u> (Mullitprecursoren) besteht bezüglich der strukturellen Nahordnung (Art und Verteilung von Kation-Sauerstoffpolyedern) eine enge strukturelle Verwandtschaft.
- Mullit bildet sich bevorzugt innerhalb der <u>*nichtkristallinen aluminiumsilikatischen Phase*</u>**.**

Der Zusammenhang zwischen Precursorstruktur und Mullitbildung ist ein wesentlicher Aspekt der vorliegenden Arbeit. Weiterhin wird die Frage diskutiert, welche Voraussetzungen zur Primärkristallisation von Mullit erfüllt sein müssen. Nichtkristalline Vorläuferphasen wandeln direkt in Mullit um, wenn

a) die chemische Homogenität hoch ist: erstmalig wurde gezeigt, daß die Ausdehnung möglicher Al_2O_3/SiO_2-Entmischungszonen $\approx$ 3nm nicht überschreiten darf

b) die Partikel der Vorläuferphase (im Fall partikulärer Gele) größer sind als $\approx$10 nm.

In allen anderen Fällen wandeln nichtkristalline Aluminiumsilikate zunächst in ein Übergangsaluminiumoxid um, welches sich bei höherer Temperatur (>1200 °C) in der verbleibenden nichtkristallinen SiO_2-Phase löst. Mit dem Erreichen einer kritischen Al_2O_3-Konzentration kommt es dann zur (sekundären) Mullitbildung innerhalb der nichtkristallinen Phase.

Generell stellt die Mullitkristallisation innerhalb der amorphen aluminiumsilikatischen Phase den typischen Bildungsmechanismus dar. Eine Ausnahme von dieser Regel ist die topotaktische Mullitbildung durch Umwandlung strukturell verwandter kristalliner Ausgangsphasen. Entsprechende Beispiele (Andalusit, X-Sialon) werden am Ende der vorliegenden Arbeit diskutiert.

Die meisten Einzelergebnisse aus den Themenkomplexen *Mullitbildung* und *Struktur nichtkristalliner Stoffe im System SiO_2-Al_2O_3* wurden in begutachteten wissenschaftlichen Zeitschriften veröffentlicht und auf internationalen Tagungen vorgestellt. Die vorliegende Habilitationsschrift basiert im Wesentlichen auf den nachfolgend aufgelisteten Publikationen. Im Anschluß an die Literaturzitate ist stichwortartig aufgeführt, welche Anteile ich zu den jeweiligen Veröffentlichungen beigetragen habe.

- M. Schmücker, W. Albers, H. Schneider, Mullite formation by reaction sintering of quartz and α-alumina - a TEM study, J. Europ. Ceram. Soc.14 (1994) 511-515
  (M.S.: Versuchsplanung, Transmissionselektronenmikroskopie, Diskussion der Ergebnisse, Erstellen der Publikation)

- M. Schmücker, H. Schneider, M. Poorteman, F. Cambier, R. Meinhold, Formatlon of Al_2O_3-rich glasses in the System SiO_2-Al_2O_3, J. Europ. Ceram Soc.15 (1995) 1201-05
  (M.S.: Mikrostrukturelle Untersuchungen, Diskussion der Ergebnisse, Erstellen der Publikation)

- M. Schmücker, H. Schneider, A new approach on the coordination of Al in non-crystalline gels and glasses of the system SiO_2-Al_2O_3, Ber. Bunsenges. Phys. Chem. 100 (1996) 1550-1553
  (M.S.: Idee, Transmissionselektronenmikroskopie, Datenanalyse, Diskussion, Erstellen der Publikation)

- M. Schmücker, K.J.D. Mackenzie, H. Schneider, R. Meinhold, NMR-studies on rapidly solidified SiO_2-Al_2O_3 -and SiO_2-Al_2O_3-Na_2O glasses, J. Non-Cryst. Solids 217 (1997) 99-105
  (M.S.: Idee, Probenherstellung, Diskussion der Ergebnisse, Erstellen der Publikation)

- M. Schmücker, H. Schneider, Sonnenofenunterstützte Forschungsarbeiten im System SiO_2 - Al_2O_3, in: Solare Chemie und Materialforschung, M. Becker, K.-H. Funken (Hrsg.) C. F. Müller Verlag, Heidelberg, 1997, 125-33
  (M.S.: Versuchsplanungen, Probenherstellung, Analyse der Ergebnisse, Erstellen der Publikation)

- M. Schmücker, H. Schneider, K.J.D Mackenzie, Mechanical amorphization of mullite and recrystallization. J. non-cryst. Solids 226 (1998) 99-103
  (M.S.: Idee, Probenherstellung, Diskussion der Ergebnisse, Erstellen der Publikation)

- M. Schmücker, H. Schneider, K.J.D. Mackenzie, M. Okuno, Comparative Al NMR and LAXS studies on Rapidly Quenched Aluminosilicate glasses J. Europ. Ceram. Soc. 19 (1999) 99-103
  (M.S.: Idee, Probenherstellung, Simulationsrechnungen, Diskussion der Ergebnisse, Erstellen der Publikation)

- M. Schmücker, H. Schneider, Structural development of single phase mullite gels, J. Sol-Gel Sci. Tech. 15 (1999a) 191-199
  (M.S.: wesentlicher Anteil beim Erstellen dieser Übersichtsarbeit)

- M. Schmücker, H. Schneider, Transformation of X-phase Sialon into mullite, J. Amer. Ceram. Soc. 82 (1999b) 1934-37
  (M.S.: Idee, Transmissionselektronenmikroskopie, Datenanalyse, Diskussion der Ergebnisse, Erstellen der Publikation)

- M. Schmücker, W. Hoffbauer, H. Schneider, Constitution and Crystallization Behaviour of Ultrathin Physical Vapor Deposited (PVD) Al_2O_3/SiO_2 Laminates, J. Europ. Ceram. Soc., 21 (2001) 2503-07
  (M.S.: Idee, Transmissionselektronenmikroskopie, Diskussion der Ergebnisse, Erstellen der Publikation)

- M. Schmücker, H. Schneider, New evidence for tetrahedral triclusters in alumino silicate glasses, J. non-cryst. Solids, 311 (2002a) 211-215
  (M.S.: Diffusionsexperimente, Rasterelektronenmikroskopie, Mikroanalytik, Diskussion der Ergebnisse, Erstellen der Publikation)

- M. Schmücker, B. Hildmann, H. Schneider, The mechanisms of 2/1- to 3/2-mullite transformation, Amer. Min. 87 (2002b) 1190-93
  (M.S.:Diffusionsexperimente, Rasterelektronenmikroskopie, Transmissionselektronenmikroskopie, Mikroanalytik, Diskussion, Erstellen der Publikation)

- M. Bartsch, B. Saruhan, M. Schmücker, H. Schneider, Novel low-temperature processing route of dense mullite ceramics by reaction sintering of amorphous SiO_2 coated γ-Al_2O_3 particle nanocomposites. J. Amer. Ceram. Soc. 82 (1999) 1388-92
  (M.S.: Transmissionselektronenmikroskopie, Beteiligung an Ergebnisdiskussion)

- K. K. Chawla, H. Schneider, M. Schmücker, Z.R. Xu, Oxide fiber/oxide matrix composites, in: Processing and design issues in high temperature materials (eds. N. S. Stoloff, R. H. Jones), The Minerals, Metals & Materials Society, Warrendale PA, 1997, 235-245
  (M.S.: Mikrostrukturelle Untersuchungen)

- R.X. Fischer, H. Schneider, M. Schmücker, Crystal structure of Al-rich mullite, Amer. Min. 79 (1994) 983-990
  (M.S.: Transmissionselektronenmikroskopie und Mikroanalytik)

- B. Hildmann, H. Schneider, M. Schmücker, High temperature behaviour of polycrystalline Alumo-sillcate fibers with mullite bulk composition: II. Kinetics of γ-Al_2O_3 -mullite transformation J. Europ. Ceram. Soc., 16 (1996) 287-92
  (M.S.: Beteiligung an Versuchsplanung und Ergebnisdiskussion)

- A. Hülsmans, M. Schmücker, W. Mader, H. Schneider, The transformation of andalusite to mullite and silica, Part I: Transformation mechanism in $[001]_A$ direction, Am. Min. 85 (2000a) 980-986
  (M.S.: Beteiligung an Versuchsplanung und experimentellen Arbeiten, Rasterelektronenmikroskopie, Beteiligung an Ergebnisdiskussion)

- A. Hülsmans, M. Schmücker, W. Mader, H. Schneider, The transformation of andalusite to mullite and silica, Part II: Transformation mechanism in $[100]_A$ and $[010]_A$ direction, Am. Min. 85 (2000b) 987-992
  (M.S.: Beteiligung an Versuchsplanung und experimentellen Arbeiten, Rasterelektronenmikroskopie, Beteiligung an Ergebnisdiskussion)

- T. Koyama, S. Hayashi, A. Yasumori, K. Okada, M. Schmücker, H. Schneider, Microstructure and mechanical properties of mullite/zirconia composites prepared from alumina and zircon under various firing conditions, J. Europ.Ceram. Soc. 16 (1996) 231-37
  (M.S.: Transmissionselektronenmikroskopie)

- K. J. D. Mackenzie, R. H. Meinhold, J. E. Patterson, H. Schneider, M. Schmücker, D. Voll, Structural evolution in gel-derived mullite precursors, J. Europ. Ceram. Soc. 16 (1996) 1299-1308
  (M.S.: Koordination der experimentellen Arbeiten, Beteiligung an Ergebnisdiskussion)

- M. Okuno, Y. Shimada, M. Schmücker, H. Schneider, W. Hoffbauer, M. Jansen, LAXS and Al-NMR studies on the temperature induced changes of non-crystalline single phase mullite precursors J. Non-Cryst. Solids 210 (1997) 41-47
  (M.S.: Koordination der experimentellen Arbeiten, Beteiligung an Ergebnisdiskussion)

- H. Schneider, M. Schmücker, K. Ikeda, W.A. Kaysser, Optically translucent mullite ceramics. J. Am. Ceram. Soc. 76 (1993a) 2912-16
  (M.S.: Transmissionselektronenmikroskopie, Diskussion der Ergebnisse)

- H. Schneider, D. Voll, B. Saruhan, M. Schmücker, T. Schaller, A. Sebald, Constitution of the γ-alumina phase in chemically produced mullite precursors, J. Europ. Ceram. Soc. 13 (1994c) 441-48
  (M.S.: Transmissionselektronenmikroskopie, Beteiligung an Ergebnisdiskussion)

- H. Schneider, M. Schmücker, J. Göring, B. Kanka, J. She, P. Mechnich, Porous alumino silicate fiber/mullite matrix composites: fabrication and properties, Ceram. Trans Vol.115, 415-434, Amer. Ceram. Soc, Westerville, OH, 2000a
  (M.S.: Mikrostrukturelle Untersuchungen, Beteiligung an Ergebnisdiskussion)

Zur besseren Übersicht sind die oben aufgeführten Literaturzitate im nachfolgenden Text durch **Fettdruck** hervorgehoben.

Danksagung

Besonderer Dank sei an dieser Stelle Herrn Prof. Dr. H. Schneider ausgesprochen. Prof. Schneider, Leiter der Abteilung *Keramische Verbund- und Funktionswerkstoffe* des DLR-Instituts für Werkstoff-Forschung, hat mir zahlreiche Kontakte zu Fachkollegen in Europa und Übersee vermittelt und mir den Freiraum gewährt, die in dieser Arbeit zusammengefassten, relativ grundlagenorientierten Fragestellungen zu bearbeiten. Sein Interesse an meinen Arbeiten und die ständige Diskussionsbereitschaft wirkten äußerst motivierend.

Herzlich bedanken möchte ich mich auch bei Prof. Dr. K.J.D. MacKenzie (New Zealand Institute for Industrial Research -IRL- und Victoria University, Wellington) für die langjährige Zusammenarbeit, die Durchführung der NMR-spektroskopischen Experimente und zahlreiche Diskussionen. Einige NMR-Untersuchungen erfolgten an der Universität Bonn im Rahmen des DFG-Sonder-forschungsbereichs 408 ("Anorganische Festkörper ohne Translationssysmmetrie"). Hier sei Herrn Dr. W. Hoffbauer Dank ausgesprochen.

Für die Berechnung der radialen Elektronendichteverteilungen aus Röntgenstreudaten danke ich Dr. M. Okuno (Universität von Kagoshima, Japan).

Die Probensynthesen erfolgten im Wesentlichen im DLR. Für die Bereitstellung von Probenmaterial und zahlreiche Hilfestellungen bedanke ich mich bei Dr. D. Voll, Dr. W. Albers, Dr. B. Saruhan, Dr. B. Hildmann, Dr. M. Bartsch, Dr. P. Mechnich, Dr. C. Taake, B. Kanka, W. Luxem, G. Paul, R. Borath und K. Baumann.

Ein besonderer Dank gilt Herrn Prof. Dr. G. Borchardt, TU Clausthal. Während eines längeren Spaziergangs am Rande einer *MULLIT*-Tagung in Schottland (ganz in der Nähe der namensgebenden Isle of *MULL*) hat mich Prof. Borchardt zur Habilitation ermuntert. Für diese Weichenstellung und den späteren Einsatz als "Habilitationsmentor" bedanke ich mich sehr.

Köln-Porz-Wahn im Juli 2003
Martin J. A. Schmücker

Contents

Abstract

Mullite is a strong candidate material for structural applications under thermal and mechanical load due to its property profile that combines high thermal and chemical stability with relatively low thermal expansion and high creep resistance. Because of these properties mullite-based fiber-reinforced CMCs are being developed at present as thermal protection systems for hot gas conducting structures in gas turbine engines.

Mullite precursor phases are most significant for the fabrication process of high-performance mullite ceramics. This is due to their high chemical purity, their high sinterability and reactivity at relatively low temperatures.

Ultrahomogeneous non-crystalline mullite precursors of type I such as aluminium silicate gels or glasses convert directly into mullite at temperatures <1000 °C by internal crystallization with high nucleation density. Structural investigations suggest close short-range order similarities between mullite and its non-crystalline counterpart. True diphasic mullite precursors of type II, on the other hand, typically consist of transition alumina phases plus vitreous silica and transform to mullite at temperatures >1200 °C. Mullite formation in diphasic starting materials is a dissolution/precipitation process: in the first step alumina dissolves in the siliceous phase, and, in the second step, mullite nucleates within the bulk of the non-crystalline siliceous phase as soon as a critical alumina concentration is reached. Type III mullite gels are non-crystalline but convert to transition alumina rather than to mullite at ≈1000 °C. Previous investigations suggested that type III gels have a lower degree of homogeneity than type I mullite precursors. To shed light on the question of chemical homogeneity and related crystallization behaviour model mullite precursors consisting of ultrathin Al_2O_3/SiO_2 multilayers were prepared by PVD techniques. Subsequent crystallization studies reveal a transition between type I (direct mullite formation) and type II characteristics (mullite formation via alumina/silica reaction) if Al_2O_3/SiO_2 layer thickness is 2-3 nm. Since nanometer-sized unmixing zones do not exist in type III precursors, as evidenced by ^{29}Si-NMR-studies, their crystallization sequence cannot be explained by a lower degree of homogeneity. TEM examination, however, revealed significantly smaller primary particles in type III gels with respect to type I gels (≈5nm vs. ≈30 nm). The conclusion is that the primary particle size of type III gels is below the size of a stable mullite nucleus but well above that of γ-Al_2O_3 and hence type III gels initially form γ-Al_2O_3 instead of mullite.

Mullite nucleation generally occurs within the bulk of a non-crystalline aluminium silicate phase. Internal mullite crystallization accounts for low nucleation barrier which is attributed to close structural relationships between non-crystalline aluminium silicates and the crystalline phase mullite, namely identical cation-oxgen polyhedra (SiO_4-tetrahedra, AlO_4-tetrahedra, AlO_6-octahedra, triclustered $(Si,Al)O_4$-tetrahedra) and similar polyhedra distribution. There are, however, exceptions from the rule of internal crystallization: In case of crystalline parent phases built of mullite-like chains of AlO_6 octahedra, topotactic mullite formation occurs. The sillimanite/mullite, andalusite/mullite, and X-SiAlON/mullite conversions confirm the idea of the transformation-controlling role of AlO_6 octahedral chains irrespective of the linking structural elements.

1. Introduction

Mullite ($\approx 3Al_2O_3 \cdot 2SiO_2$) is one of the most widely studied ceramic materials. This is due to the fact that mullite is not only a major constituent of traditional, clay-based ceramics, but plays an increasing role as an advanced ceramic material for high-temperature structural applications (Aksay et al., 1991, Schneider et al., 1994a). Moreover, mullite has gained some popularity as a functional ceramic material e.g as a substrate in high performance packaging applications (Kanzaki, 1990) or as a an optical window material in the mid-infrared portion of the spectrum (Musikant, 1981, Gentilman, 1986, **Schneider et al., 1993a**).

Mullite is a strong candidate material for structural applications under thermal and mechanical load due to its property profile that combines high thermal and chemical stability with a relatively low thermal expansion coefficient (3 - 7 ppm/K, Schneider and Eberhard, 1990) and high creep resistance (Dokko, 1977). The main drawback of monolithic mullite ceramics, however, is its inherent brittleness. Many efforts were made during the last two decades to overcome this problem by reinforcing mullite matrices: to achieve tough and damage tolerant mullite ceramics reinforcing components such as ZrO_2 particles (e.g. **Koyama et al., 1996**), whiskers or chopped fibers (e.g. Hirata et al., 1991), and continuous fibers were employed, the latter being the most promising. Various approaches focused on the microstructural design of long fiber reinforced ceramics were published in the 1990´s (e.g. Iwata et al., 1989, **Chawla et al., 1997**, **Schneider et al., 2000a**). Potential near future applications of fiber-reinforced mullite CMCs are components of gas turbine engines (thermal protection systems for combustors, liners, diffusor rings), burner tubes, substrates for catalysts, filters, and kiln furniture.

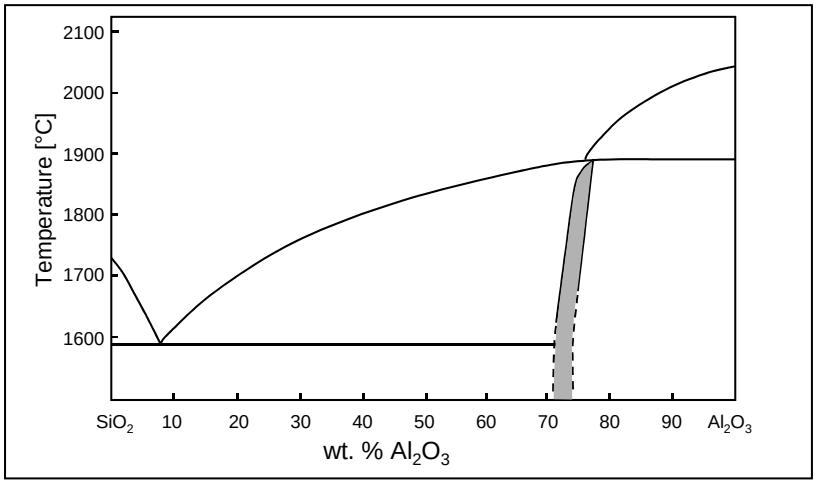

Fig. 1: SiO_2-Al_2O_3 phase diagram after Klug et al. (1997). Grey area: mullite solid solution region

Mullite is the only stable binary phase of the system Al_2O_3-SiO_2 existing at ambient conditions (Klug et al., 1987, Fig. 1). Its crystal structure is composed of chains of aluminium oxygen octahedra running parallel to the crystallographic c-axis. Octahedral chains are cross linked by AlO_4 and SiO_4 tetrahedra occurring in dimers and trimers. Relatively big voids exist in the mullite

structure caused by structural oxygen vacancies inducing a shift of the adjacent Al atoms (Al*, see Fig. 2). The general formula of mullite composition is Al_2 $[Al_{2+2x}$ $Si_{2-2x}]$ O_{10-x} (Angel and Prewitt, 1986), where x denotes the number of vacancies formed by the exsolution of O(c) oxygen atoms (Fig. 2).

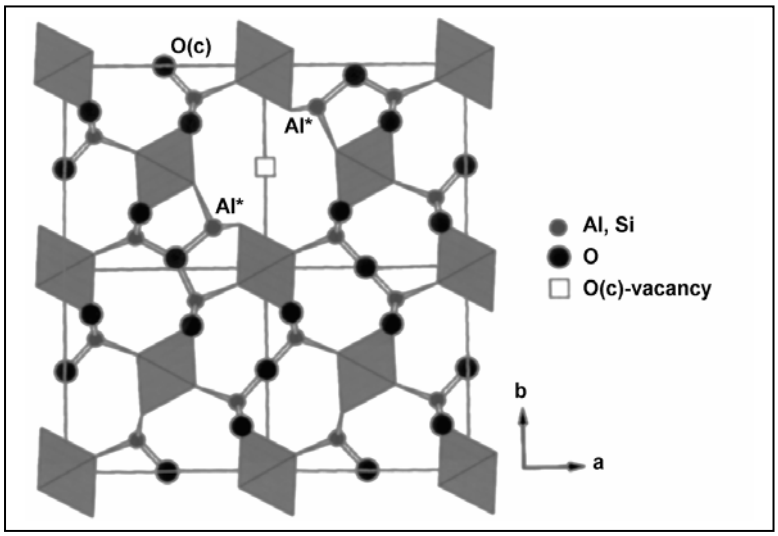

Fig. 2: Crystal structure of mullite in a projection down the c-axis (after Angel and Prewitt, 1986). Four unit cells are plotted.

Mullite precursor phases are most significant for the fabrication process of high-performance mullite ceramics. Instead of mineral raw materials synthetic mullite precursors have been increasingly used as starting powders if high chemical purity, high sinterability and mullitization at relatively low temperatures is required. For low-temperature mullite formation, precursor phases with colloidal or even molecular cation mixing have been developed, taking into account that diffusion-controlled processes are relatively sluggish in the system SiO_2-Al_2O_3. Thus, for instance, temperatures above 1700 °C are required for complete mullitization of a micron-sized admixture of α- Al_2O_3 and quartz. A relatively low diffusion and reaction rate occurring in the pure SiO_2-Al_2O_3 system is just the other side of the high-temperature stability of mullite mentioned above.

Though mullite is the only stable product in the reaction between SiO_2 and Al_2O_3 the mullite formation history is strongly affected by the constitution and structure of the respective precursor phase. Therefore, profound knowledge of the precursors´ transformation behaviour allows the design of a tailored precursor phase that determines the resulting mullite microstructure and its properties. As an example, mullite ceramics, designated for structural applications at moderate temperatures should have a microstructure with small crystal size and a minimum amount of pores while small amounts of glassy phase can be accepted. In contrast, mullite ceramics provided for high temperature structural applications have to be glass-free and a somewhat greater crystal size is favored. Moreover, mullite matrices of fiber-reinforced ceramics must be synthesized at low temperatures (to avoid fiber degradation) while optical window materials may be fabricated at high temperatures to achieve dense ceramics with only few grain boundaries. Thus, the precursor

phases provided for the different materials have to be optimized with respect to either mullite formation rate, sinterability, composition, or additives.

It is generally accepted, that two prototypes of mullite precursors do exist (e. g. Okada et al., 1991): One type shows direct mullitization from the amorphous state at temperatures as low as ≈950 °C, while the other type shows mullitization only above 1200 °C by reaction of transient spinel-type alumina with silica. The former precursor type is designated as single phase (Hoffman et al., 1984), polymeric (Yoldas, 1990) or type I precursors (Schneider et al., 1993b) while the latter one is called diphasic, colloidal, type II, or NM (no mixing, Okada et al., 1986). The type of mullite precursor depends on the starting material and on the preparation conditions. Colloidal suspensions of Al- and Si-compounds lead to diphasic precursors, whereas true solutions of salts or organometallic compounds may give rise to single phase precursors. However, homogeneous solutions of the starting compounds can also produce diphasic mullite precursors. Thus, for instance, ethanol diluted admixtures of tetraethylorthosilane plus aluminium-sec-butylate were reported to result in single or diphasic gels, respectively, depending on the process route (Schneider et al.,1993b, Voll, 1995).

The present paper gives an overview on mullite precursor phases and on their thermal transformation behaviour. The main emphasis is on the structure (atomic arrangement, short-range-order) of the non-crystalline aluminium silicate phases, on the structural development before mullitization, on the correlation between precursor homogeneity and crystallization history, and on the mechanisms of mullite formation.

2. Precursors transforming directly to mullite at temperatures below 1000 °C (Type I)

In numerous papers mullite precursors transforming directly to mullite at temperatures below 1000 °C were considered to be single phase (e.g. Hoffmann et al., 1984). In more recent studies, however, the single phase character of this precursor type was called into question: Huling and Messing (1992) pointed out that spinodal phase separation in the amorphous state may precede mullite crystallization, while Okada et al. (1996) and **Schmücker et al. (2001)** showed that even diphasic mullite precursors may directly transform to mullite at low temperatures under special circumstances. None the less, cation mixing on atomic level, i. e. occurrence of Al-O-Si sequences in general can be assumed for mullite precursors transforming to mullite below 1000 °C. Thus, in the following this type of mullite precursor will be called ultrahomogeneous or type I according to Schneider´s nomenclature (Schneider et al., 1993b).

2.1. Preparation of ultrahomogenoeus (type I) mullite precursors

There are various kinds of type I mullite precursors depending on their preparation route: mullite precursors prepared by chemical methods, such as sol-gel techniques, co-precipitation, and spray hydrolysis, are the most significant from a technological point of view. Aluminium silicate glasses with mullite composition can be regarded as type I mullite precursors as well since the structural short-range order and the crystallization behaviour of these glasses and of the corresponding gels is virtually the same. Preparation of mullite glasses, however, is difficult since the glass forming ability of aluminium silicate melts is low and hence high quenching rates are required to suppress crystallization. More recently it was shown that ultrahomogeneous mullite precursor phases can also be prepared by vapour deposition techniques, such as HF-sputtering (**Schmücker, unpublished results**, Taake, 1999). In addition, non-crystalline aluminium silicate powders with atomic short-range order similar to mullite gels and glasses can be prepared by mechanical amorphization of mullite carried out by long-term ball milling (**Schmücker et al., 1998**). Thus, the starting materials of ultrahomogeneous non-crystalline aluminium silicates can be a liquid phase (solution, melt), vapour phase or crystalline solid phase as sketched in Fig. 3.

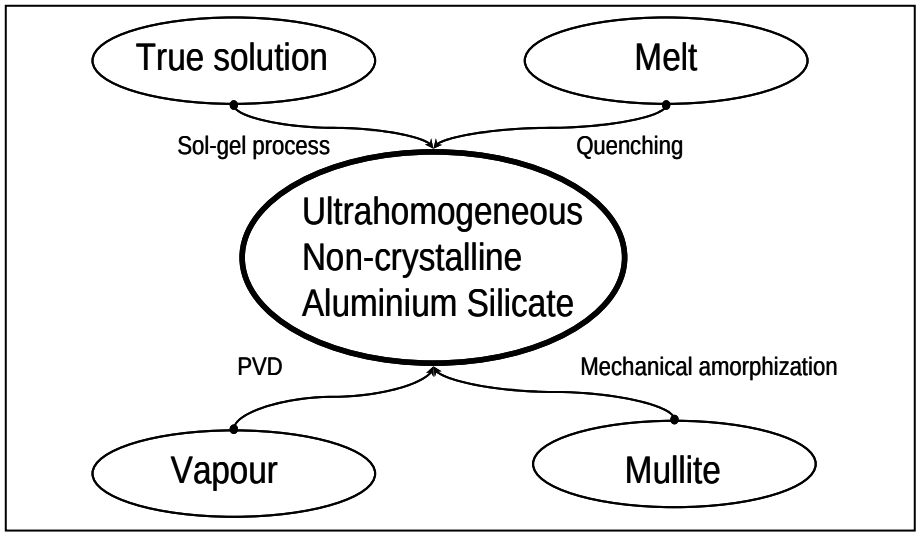

Fig. 3: Flow chart showing starting materials and processes leading to ultrahomogeneous non-crystalline mullite precursor phases.

Preparation of ultra homogeneous mullite precursors by chemical methods

Many approaches to synthesize highly homogeneous mullite precursor phases have been reported. In general, in the first step a true solution containing the Al- and Si species has to be prepared and in the second step the homogeneous cation distribution of the solution is transformed into the solid state by a precipitation or condensation process. A comprehensive overview of methods and techniques leading to type I mullite precursors is given by Schneider (1994a) and Voll (1995). In the following some fundamental works are briefly summarized:

A mullite precursor forming mullite below 1000 °C was reported by Ossaka (1961): This precursor phase was prepared by dissolving sodium silicate and potassium alum in sulphuric acid. Addition of hexamethylenetetramine gave aluminium silicate precipitates which were filtered and washed to remove residual alkali and amine components. The main disadvantage of this process, however, is the poor yield of aluminium silicate precipitates and the existence of residual alkali ions.

The sol-gel method starting with an organometallic Si-source was introduced by Hoffman et al. (1984) for the preparation of a type I mullite precursor: A solution of TEOS ($Si(OC_2H_5)_4$ and $Al(NO_3)_3{\cdot}9H_2O$ (ANN) in ethanol was gelled at 60 °C within several days by a hydrolysis-polymerization reaction. The mullite precursor derived by this method was called "single phase xerogel". A similar process was used by Okada and Otsuka (1986). It was emphasized that the aluminium silicate gel transforms directly to mullite only in case of slow hydrolysis ("SH xerogel"). Rapid hydrolysis, on the other hand, results in a gel that forms transition alumina rather than mullite as the first crystalline phase. The same is true if the gels are aged for more than 1 month (Okada and Otsuka,1990), or if gelation is carried out at temperatures below 60 °C (Okada,1996).

Mullite precursor preparation by hydrolysis methods using organometallic compounds of both constituents, Si and Al, was also reported by many authors. Alcoholates such as aluminium-isopropylate or aluminium-sec.-butylate and tetraethylorthosilane (TEOS) or tetramethylorthosilane (TMOS) have been used as starting materials. However, the preparation of ultra-homogeneous type I precursors from alkoxides of Al and Si is difficult and very sensitive to the reaction conditions. This is due to the different rates of hydrolysis and polycondensation of the starting compounds which may cause demixing effects. To circumvent the problems arising from the different reactivities of aluminium and silicon species during the sol-gel process various methods have been reported for the preparation of single phase mullite precursors:

- very slow hydrolysis, e.g. by ambient humidity (Yoldas, 1990, Okada and Otsuka, 1986, Colomban, 1989)
- prehydrolysis of Si (Voll, 1995)
- Reactivity reduction of the Al-alkoxide using β-diketone (e.g. acetylacetone), as a chelating agent (Heinrich and Raether, 1992)

Spray-drying or spray-pyrolysis is used as an alternative method to the hydolysis-based sol-gel process. Spraying small droplets of a solution of Al and Si-compounds into a hot reaction chamber leads simultaneously to evaporation of the solvents, thermal decomposition and polymerization of the compounds. By the rapid reaction process demixing effects can be suppressed. Small droplets, prepared by atomizers or ultrasonicators, result in powders of spherical shape with

(sub)micrometer size. Kanzaki et al. (1985) were the first authors to report ultra-homogeneous mullite precursors prepared by spray pyrolysis: TEOS and aluminium nitrate were dissolved in a water-methanol solution, atomized, and subsequently sprayed into a furnace heated at 350-650 °C.

Preparation of glasses with mullite composition

Gani and McPherson (1977a) showed that aluminium silicate glasses with mullite composition can be used as a suitable precursor of mullite ceramics. However, the glass forming ability of aluminium silicate melts with alumina contents >20 % is low. Therefore, high cooling rates are required to suppress crystallization of the melt during the cooling process. Essentially, two methods of mullite glass preparation were used: Quenching of small melt droplets produced by flame spheroidisation techniques (Takamori and Roy, 1973), plasma spraying (Gani and McPherson 1977b), or melt atomization (Morikawa et al., 1982) in water or, alternatively, by splat cooling of the melts between two rollers made of steel (Macdowell and Beall, 1969), titanium (Risbud et al. 1987) or aluminium (**Schmücker et al., 1997**). The glass forming studies revealed that crystallization of melts with mullitic composition can be suppressed only if particle size or flake thickness is below ≈20 µm (Gani and McPherson, 1977b, **Schmücker et al., 1995**, **Schmücker and Schneider, 1997**). Evidence suggested that the critical particle size or the glass flake thickness, respectively, is controlled by the thermal conductivity within the supercooled melt, rather than by the cooling medium. Fig. 4 shows a rapidly solidified aluminium silicate flake produced by roller quenching. Thin areas are transparent and non-crystalline while thicker areas appear white due to light scattering on micron-sized mullite crystals formed during the cooling process.

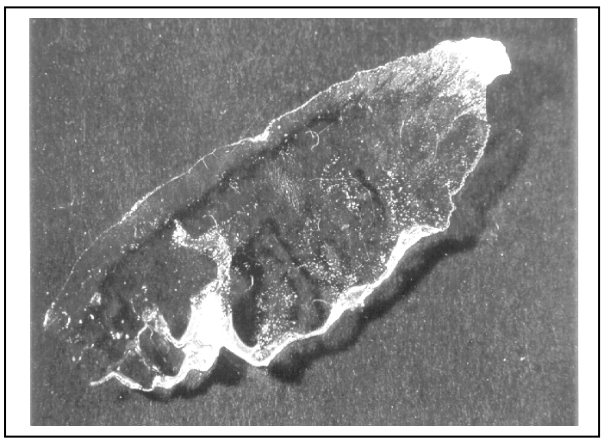

Fig. 4: Rapidly solidified aluminium silicate glass prepared by roller quenching. Thin and transparent areas are vitreous while thicker flake areas are partially crystalline due to insufficient cooling rate.

2. 2. Structural development of type I mullite gels before crystallization

Wet stage

Little information exists about the structural development during hydrolysis and gelation ("wet stage"): Fukuoka et al. (1993) investigated the Al coordination of sols and wet gels derived from TEOS plus various Al-sources by means of ^{27}Al-NMR spectroscopy: According to these studies only AlO_6 occurred in Si-Al sols and wet gels derived from aluminium nitrate nonahydrate (ANN) and from boehmite sol while AlO_4 plus AlO_6 was determined when aluminium formoacetate was used. AlO_4-, AlO_5-, and AlO_6-polyhedra, on the other hand, were postulated in gels derived from aluminium di-(butoxide)-ethylacetoacetic ester chelate. Pouxviel and Boilot (1989) investigated early gelation stages of Si-Al-esters. Small angle X-ray scattering (SAXS) revealed aggregation of 5 to 8 Å sized elementary clusters. In the case of precursors derived from TEOS plus Al-sec-butylate using acetylacetone as chelating agent primary particles of 21 to 34 Å were determined and the condensation behaviour was found to be a reaction limited cluster-cluster aggregation (Pouxviel et al., 1987). Particles of similar size (ca. 20 Å) have been observed in aluminium nitrate / TEOS derived sols by means of dynamic light scattering (Jaymes and Douy, 1996).

Dried gels

The development of dried mullite gels prior to crystallization was investigated in detail during the last decade (e.g. **Schmücker and Schneider, 1999a**): investigations were focussed on size and development of primary particles, on volatilization of H_2O and organic groups, on the condensation of the network, and on changes in the kind and frequency distribution of Al-O polyhedra.

By means of high-resolution scanning electron microscopy, submicron-sized particles become visible in dried or calcined aluminium silicate gels. Fig. 5 shows the fractured surface of a dried gel (150 °C) derived from slow hydrolysis of TEOS/Al-sec-butylate solutions. The SEM micrograph reveals 20-50 nm sized spherulites with a relatively uniform size distribution. Gels calcined at higher temperatures (up to 800 °C) do not indicate a significant change in particle size and agglomeration behaviour. This finding is in good accordance with measurements of the gel´s density; density data calculated from the respective refractive indices reveal that only a 7% gain in density is obtained after calcination at 900 °C with respect to gels dried at 150 °C (**Okuno et al., 1997**). Similar findings were reported by Li and Thomson (1990): a BET surface area of 150 m^2/g was determined in mullitic gels derived from TEOS plus ANN after drying at 300 °C. Further calcination (<900°C) does not reduce the BET surface or the corresponding size of primary particles (≈20 nm).

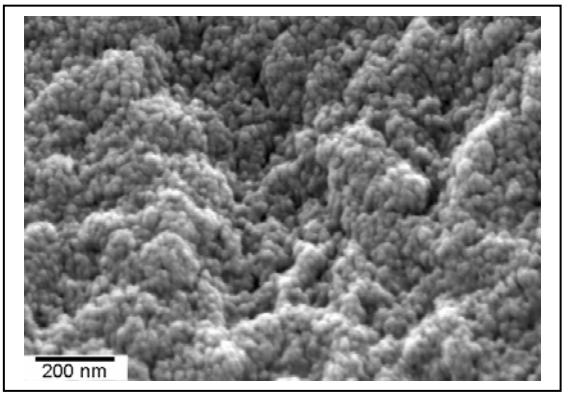

Fig. 5: Scanning electron micrograph of type I gel showing spherical particles of 20-50 nm in size.
(Schmücker, unpublished)

Dehydration and condensation of mullite gels

Temperature-dependent removal of H_2O, hydroxyl groups and organic residuals has been investigated systematically by means of Fourier transform infrared studies (FTIR) and mass spectrometry (Voll et al., 1998, **MacKenzie et al., 1996**). Fig. 6 shows the analytically determined water loss of TEOS/Al-sec-butylate-derived single phase gels as a function of calcination temperature together with the integral absorbances of H_2O and OH^-. Up to annealing temperatures of ≈600 °C mullite gels loose virtually all molecular H_2O which is weakly bound at the gel surface and in open pores, whereas the stronger, structurally bound OH^- groups are not much affected. At temperatures > 700 °C thermal energy is sufficient for dehydroxylation and for subsequent recombination of OH^- groups to H_2O. The newly formed H_2O does not evaporate immediately as can be seen from the temporary increase of the H_2O absorption band, suggesting that H_2O is trapped in nanopores and significant evaporation will not take place before the calcination temperature reaches 800 °C. Above about 800 °C diffusion of H_2O molecules through the gel network is possible with the consequence that at 900 °C the mullite precursors are nearly H_2O-free.

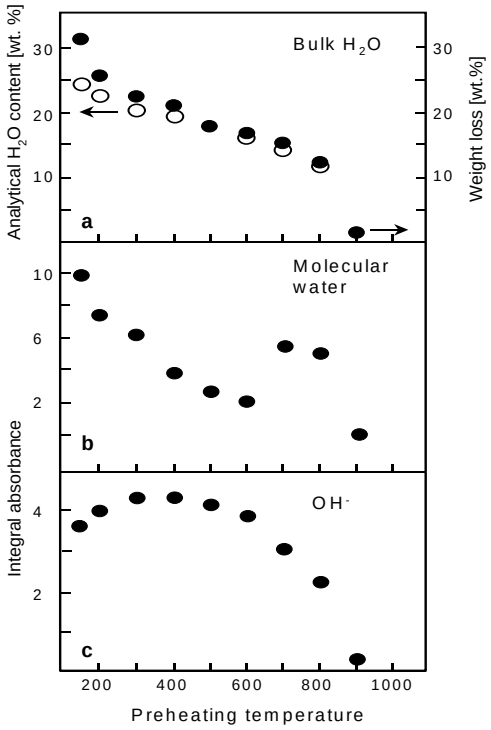

Fig. 6: Temperature-induced dehydroxylation of single phase (type I) mullite gels: (a) Analytical H_2O contents; open circles: moisture evolution analysis (MEA), full circles: Thermobalance (TG); (b) Integral absorbance values of the H_2O combination band centered at 5160 cm^{-1}; (c) Integral absorbance values of the (Si,Al)-OH combination band at 4540 cm^{-1}. Data from Voll et al. (1998)

Investigations of the temperature-dependent decomposition and combustion of organic residuals performed by means of in-situ mass spectrometry reveal that organic species are retained in mullite gels up to high temperatures (900 °C under dynamic heating conditions). Released residual organic species formed by prolonged heating below ≈ 250 °C are predominantly straight chains or cyclic hydrocarbons, whereas heating at ≈ 350 °C leads to their conversion into aromatic species. Prolonged heating above 350 °C gradually destroys the aromatic species by oxidation (**MacKenzie et al., 1996**).

^{29}Si NMR investigations have been used to document the temperature-induced condensation of the gel´s network (Schneider et al., 1992, **MacKenzie et al., 1996**). Fig. 7 shows a series of ^{29}Si NMR spectra of calcined aluminium silicate gels prepared by slow hydolysis of TEOS and Al-sec.-butylate. The spectra contain a major resonance centered at about -88 ppm and two broad shoulders at ≈-55 and ≈-110 ppm, respectively. The spectral region around -88 ppm is typical for tetrahedrally coordinated Si in aluminium silicates such as mullite or mullite glasses (Risbud et al., 1987, Schneider et al., 1992). The broad shoulder at –110 to -115 ppm, usually hardly visible in type I mullite gels and glasses, indicates the presence of silica-rich domains, while the -55 ppm signal is attributed to residual organo-silicon species and to their transient combustion products (**MacKenzie et al., 1996**).

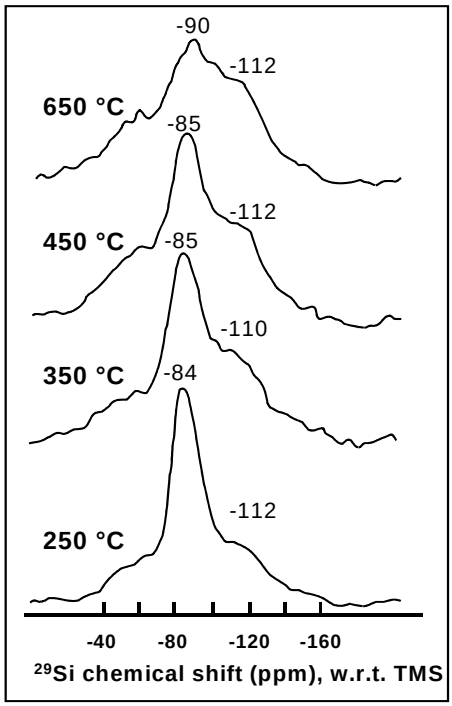

*Fig. 7: ^{29}Si NMR spectra of ultrahomogeneous (type I) mullite gels heat-treated at different temperatures prior to crystallization. Data from **MacKenzie et al. (1996)**.*

The temperature-dependent increase of the -110 ppm signal may reflect gradual demixing of the gel in silica-rich and alumina-rich domains (e.g. Huling and Messing, 1992, see below). The major resonance, on the other hand, shows a slight but significant up-field shift from about

-84 ppm (250 °C) to -91 ppm (650 °C). According to Mägi et al (1984) and Engelhardt and Michel (1987) an up-field peak shift in the ^{29}Si-NMR spectrum of aluminium silicates can be explained either by a decreasing number of next nearest Al atoms around Si or by an increasing number of bridged (Al,Si)-O-(Si,Al) oxygen atoms. Since the major resonance position of the gel approaches the position of corresponding aluminium silicate glasses (e.g. **Schmücker et al., 1997**) it can be assumed that the temperature-induced upfield shift reflects a gradual condensation process of the gel network accompanied by the evaporation of volatile compounds. Little increase of the gel density during calcination (see above) indicates that the overall porosity is not dramatically reduced by the network condensation process, and hence a relatively rigid oxide skeleton will be formed in an early stage of the precursor development.

Calculations of radial distribution functions (RDF) have provided further evidence for a temperature-induced condensation of the network of aluminosilicate gels. As-prepared (150 °C) mullite type I precursors yielded RDF-patterns with a prominent peak at 1.8 Å, and broad peaks of low intensity near 2.9 Å, 3.2 Å, and 4.2 Å (Fig. 8). On the basis of the ion radii of Al^{3+}, Si^{4+}, and of 0^{2-}, the peak near 1.8 Å was ascribed to T-O (T = Al^{3+}, Si^{4+}) atomic pairs, whereas those at 2.9 Å, 3.2 Å, and 4.2 Å were associated with O-O, T-T (i.e.: T(1)-O(1)-T(2)), and T-O(2) (i.e.: T(1)-O(1)-T(2)-O(2)) pairs. The maxima near 3.2 Å and 4.2 Å gradually become more intense with heat treatment. This again was interpreted as an increasing condensation of the precursor network (**Okuno et al., 1997**)

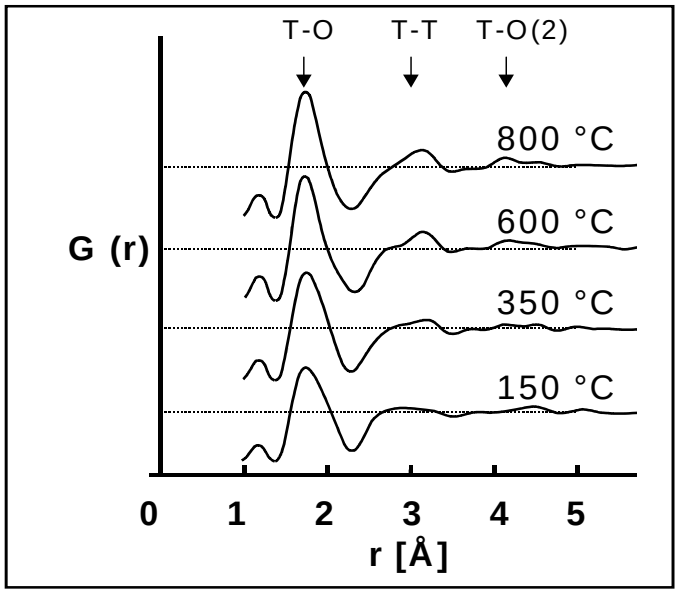

Fig. 8 : Pair distribution functions of ultrahomogeneous (type I) gels heat-treated at different temperatures prior to crystallization. Data from ***Okuno et al. (1997)****.*

^{27}Al NMR spectroscopy provides information on the mode and distribution of Al-O-polyhedra in aluminium silicate gels. Ultrahomogeneous mullite precursors display ^{27}Al NMR spectra with 3 peaks centered near 0, 30, and 60 ppm, (Fig. 9). In the as-dried gel (150°C), the 0 ppm signal is stronger

than the 60 ppm signal, while the 30 ppm peak is very weak. With heat-treatment, a strong increase in the 30 ppm signal intensity is observed, approaching a spectrum very similar to those of Al_2O_3-SiO_2 glasses. ^{27}Al NMR data on glasses of the system Al_2O_3-SiO_2 was first published by Risbud et al. (1987). They assigned the ^{27}Al NMR signals near 0 ppm and 60 ppm to octahedral Al ($Al^{[6]}$) and to tetrahedral Al ($Al^{[4]}$), respectively. The 30 ppm resonance was attributed to fivefold coordinated Al ($Al^{[5]}$) due to the intermediate position between those of $Al^{[6]}$ and $Al^{[4]}$, and due to the fact that it exhibits a chemical shift similar to the isotropic shift of andalusite [#§]. A large number of NMR studies carried out on aluminium silicate gels and glasses referred to the paper of Risbud et al., and mentioned the presence of $Al^{[4]}$, $Al^{[5]}$, and $Al^{[6]}$ in these materials. However, the assignment of the 30 ppm resonance in the ^{27}Al NMR spectrum is not undisputed (see below).

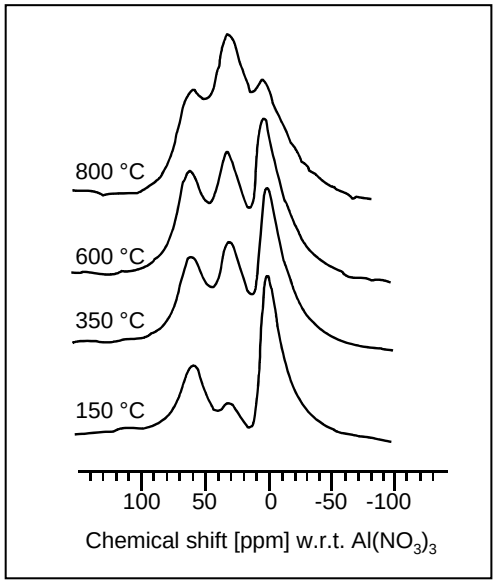

Fig. 9 : ^{27}Al NMR spectra of ultrahomogeneous (type I) mullite gels heat-treated at different temperatures prior to crystallization. Data from ***Schmücker and Schneider (1996)****.*

Geradin et al. (1994) and Schneider et al. (1994b) pointed out that there must be a correlation between the 30 ppm NMR signal and mullite formation: If Al sites corresponding to the 30 ppm signal are predominant, mullite formation is preferred to transition alumina crystallization or, in other words, the intensity of the 30 ppm peak in sol-gel derived mullite precursors is assumed to correlate with their degree of structural homogeneity. Taylor and Holland (1993), on the other hand, reported that aluminium is tetrahedrally coordinated in very homogeneous gels, while diphasic gels are characterized by high amounts of octahedrally coordinated Al. Fivefold coordinated Al was believed to occur in interfacial regions between homogeneous and less homogeneous domains.

[#§] Andalusite contains AlO_6 octahedra chains running parallel to the c-axis. These octahedral chains are connected by double chains consisting of AlO_4 tetrahedra and AlO_5 polyhedra (Burnham and Buerger, 1961).

Coordination of Aluminium in calcined gels and glasses of the system SiO_2-Al_2O_3

The structure of gels and glasses in the system SiO_2-Al_2O_3, namely the coordination of Al, has been a point of interest for many years. In the 1960´s, Lacy (1963) assumed on the basis of charge balance considerations that triclusters of cation-oxygen tetrahedra (i.e. 3 tetrahedra linked together by one common oxygen atom) are formed, if Si is partially replaced by Al in melts and glasses. 25 years later, however, with the introduction of MAS NMR spectroscopy another structural model became popular. In the pioneering work of Risbud et al. (1987) three ^{27}Al MAS NMR signals were observed centered at 0, 60 and 30 ppm. The resonances were attributed to Al-O-polyhedra in octahedrally ($Al^{[6]}$), tetrahedrally ($Al^{[4]}$) and fivefold coordination, respectively (see above). Meinhold et al. (1993), on the other hand, attributed the 30 ppm peak to $Al^{[4]}$ with elongated Al-O bonds rather than to $Al^{[5]}$. This suggestion was obtained on the basis of ^{27}Al NMR line shape analyses together with RDF and EXAFS data. Today, the assignment of the 30 ppm resonance is still a point of controversy: Bodart et al. (1999) supported the idea of the presence of five-fold coordinated AlO_5 polyhedra on the basis of recent multiple quantum ^{27}Al NMR studies, while other authors provided evidence for the model of distorted tetrahedra (Peeters et al., 1997). According to McManus et al. (2001) the experimental data do not allow the questionable resonance to be assigned unambiguously.

Schmücker and Schneider (1996) have reactivated Lacy´s model of oxygen-sharing tetrahedral triclusters. Starting from the observation that mullite is formed within the bulk of aluminosilicate gels or glasses in extremely high nucleation densities (Fig. 10), short-range order similarities were postulated between mullite and its non-crystalline counterpart. Since no $Al^{[5]}$ but tetrahedral triclusters exist in the mullite structure, it was argued that $(Si,Al)O_4$-triclusters rather than AlO_5 polyhedra exist in aluminosilicate gels and glasses.

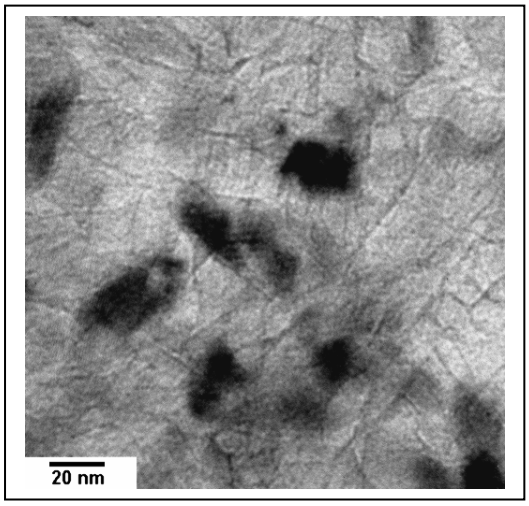

Fig. 10: Mullite crystals formed after calcination of aluminium silicate glass. Crystallite size of 20-30 nm accounts for high nucleation density ***(Schmücker, unpublished)***

Short-range order similarities between non-crystalline aluminium silicates and mullite are also reflected by similar ^{27}Al NMR spectra (Fig. 11). Two different $Al^{[4]}$ sites in mullite cause a splitting of the ^{27}Al NMR signal into two peaks at ≈60 ppm and ≈43 ppm, the latter being attributed to

tricluster forming Al* sites (Merwin et al., 1991, see also Fig. 2). The intense upfield shift of the Al* resonance in mullite is close to the 30-35 ppm signal occurring in amorphous aluminium silicates, which therefore actually may be attributed to triclustered AlO_4 tetrahedra.

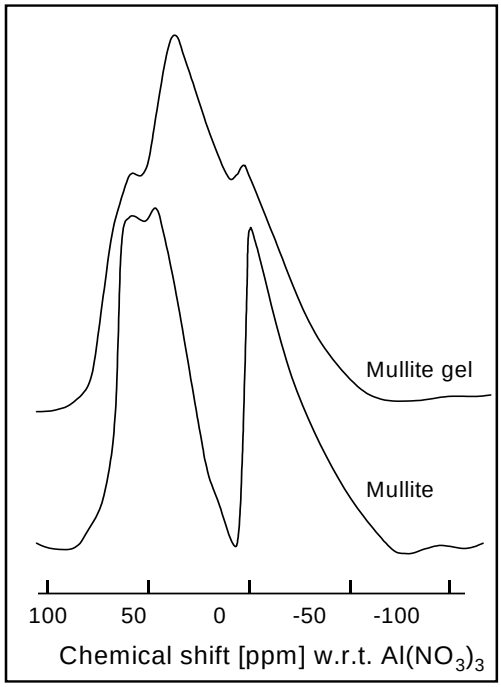

Fig. 11: ^{27}Al NMR spectra of ultrahomogeneous (type I) mullite gels and mullite. Data from ***Schmücker and Schneider (1996).***

The combination of NMR data and pair distribution functions (PDF) of aluminium silicate glasses with 35, 50 and 60 mol% Al_2O_3 also speaks against AlO_5 polyhedra as a predominant species (**Schmücker et al., 1999**): ^{27}Al NMR spectral deconvolution signalizes that ≈20 % of the observed Al occurs in tetrahedral sites, ≈55% corresponds to the 30 ppm signal and ≈25 % of the Al is sixfold coordinated. Table1 presents the mean coordination numbers of different glasses according to model 1 ($Si^{[4]}$ plus 20% of total Al in fourfold, 55% in five-fold, and 25% in six-fold coordination) and to model 2 ($Si^{[4]}$ plus 75% of total Al in fourfold and 25% in six-fold coordination) in comparison with coordination numbers obtained from PDF data. Coordination numbers calculated on the basis of model 1 (with $Al^{[5]}$) are far greater than values obtained from X-ray data, while mean coordination numbers calculated from model 2 (without $Al^{[5]}$) are much closer to the values resulting from the PDFs.

Glass composition (mol% Al_2O_3)	Model 1 (AlO_4, AlO_5, AlO_6)	Model 2 (AlO_4, AlO_6)	Calculated from PDF
60	4.80	4.38	4.3
50	4.70	4.33	4.2
35	4.54	4.26	4.1

*Table 1: Mean cation coordination number derived from models 1 and 2 compared with values derived from PDF data (****Schmücker et al., 1999****).*

In the next step **Schmücker et al.** fitted the first PDF maxima of the glasses to either 4 gaussian functions according to model 1 ($Si^{[4]}$-O, $Al^{[4]}$-O, $Al^{[5]}$-O, $Al^{[6]}$-O) or with 3 gaussian functions according to model 2 ($Si^{[4]}$-O, $Al^{[4]}$-O, $Al^{[6]}$-O). Using interatomic distances, calculated from ionic radii and the site fractions derived from the NMR spectra, the only fitting parameters were those associated with the standard deviation of the respective gaussian functions and a global parameter fitting the sum of the individual normal functions to the PDF profile. The calculations clearly showed that PDF data can be fitted well for all three glass compositions by taking into account only AlO_4 and AlO_6 polyhedra in addition to SiO_4. On the other hand, if $Al^{[5]}$ is related to the 30 ppm peak, and included in the fitting procedure, the shapes of the PDFs and the calculated distance distributions match poorly. Fig. 12 shows the simulation of the first PDF profile of the glass with 60 mol% Al_2O_3.

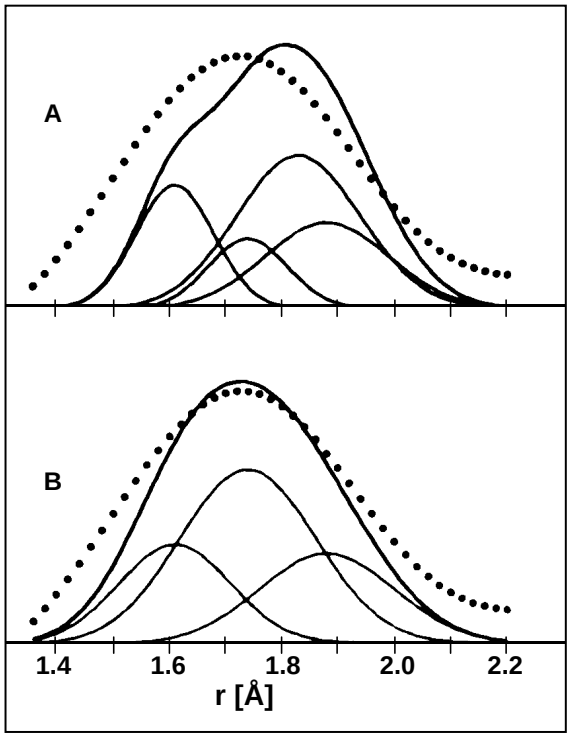

Fig. 12: Simulation of the first PDF maximum of mullite glass by 4 (A) and by 3 (B) gaussian functions corresponding to ($Si^{[4]}$-O, $Al^{[4]}$-O, $Al^{[5]}$-O, $Al^{[6]}$-O) distances, and ($Si^{[4]}$-O, $Al^{[4]}$-O, $Al^{[6]}$-O) distances, respectively. Data from ***Schmücker et al. (1999).***

Another fitting strategy was used for the first PDF maxima of Type I gels calcined at different temperatures (Fig. 8, **Schmücker and Schneider, 1996**). The respective first PDF maxima were fitted to two normal functions without parameter constraints (Fig. 13). The following conclusions can be drawn from the positions and intensities of the calculated normal functions: position of function 1 (maximum at 1.69 Å) corresponds exactly to the mean tetrahedral (Al,Si)-O distance in mullite (Saalfeld and Guse, 1981). Its relative intensity increases with the calcination temperature which implies a gradual increase of the relative amount of tetrahedrally coordinated Al. The intensity of the second normal function decreases with annealing temperature, and the peak maximum position shifts from 1.95 to 1.89 Å. The 1.89 Å distance is typical for $Al^{[6]}$-O bond lengths in crystalline aluminium silicates (Saalfeld and Guse, 1981), while the elongated 1.95 Å distance in

the 150 °C and 350 °C samples may rather be attributed to Al-OH bonds. The ratio of $(Si,Al)^{[4]}$ to $Al^{[6]}$ changes slightly from ≈60/40 at 150 °C to ≈70/30 at 600 and 800 °C. Thus, the ratio of tetrahedral to octahedral coordinated cations of the calcined gels is very similar to that of mullite (67/33). The increase of fourfold coordinated cations with the calcination temperature corresponds to the tendency noted in the NMR spectral development (Fig. 9), provided the 30 ppm signal is attributed to $Al^{[4]}$.

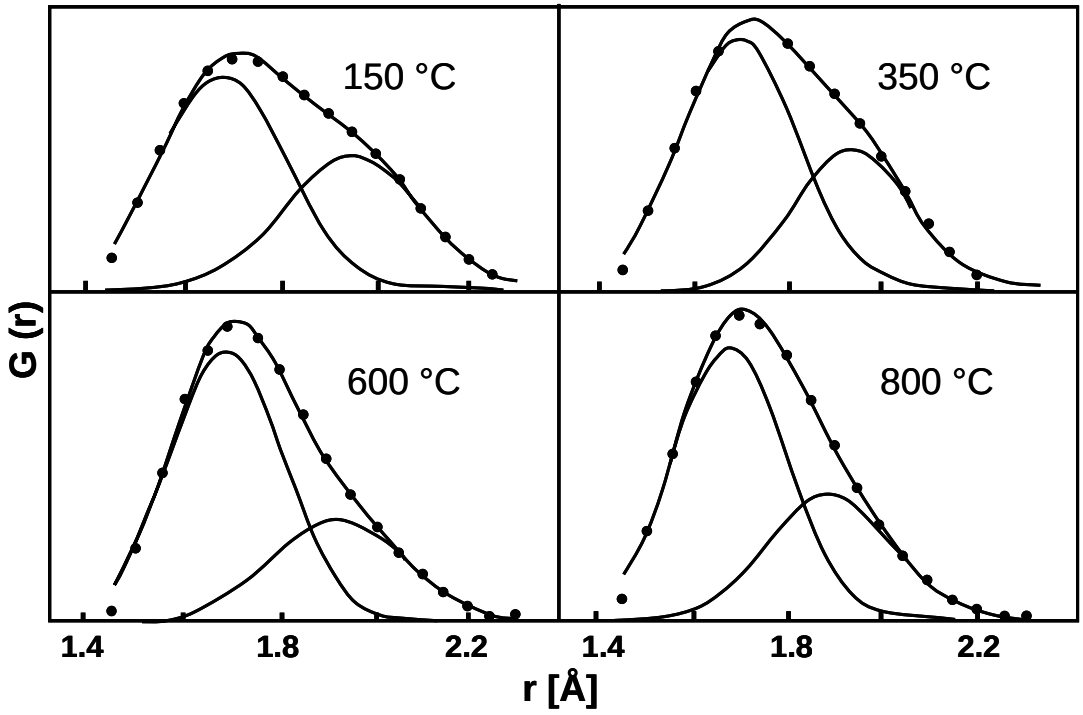

Fig. 13: Simulation of the first PDF maximum of mullite gels heat-treated at different temperatures. Data from ***Schmücker and Schneider (1996).***

The assignment of the 30 ppm resonance to AlO_4 tetrahedra and Lacy´s charge balance considerations are self-consistent. **Schmücker et al. (1997)** showed that a reciprocal dependency exists between the 30 ppm signal intensity and the Na^+ content in glasses of the system SiO_2-Al_2O_3-Na_2O suggesting that tricluster formation and incorporation of alkali ions are competitive mechanisms to achieve charge neutrality (Fig. 14). Similar findings were reported from gels of the system SiO_2-Al_2O_3-Na_2O (Taake, 1999).

More recently, it was shown that Na addition to aluminium silicate glasses/melts has a strong influence on mullite nucleation (**Schmücker and Schneider, 2002a**). Fig. 15 shows reaction couples consisting of an alumina-rich mullite single crystal (Al_2O_3/SiO_2 ≈ 2/1) and aluminium silicate glasses with and without Na addition after firing at 1650 °C. While stoichiometric mullite (Al_2O_3/SiO_2 = 3/2) nucleates within the virtually pure SiO_2-Al_2O_3 melt (see also **Schmücker et al., 2002b**), 3/2-mullite forms epitactically at the surface of the parent 2/1-mullite crystal if the aluminium silicate melt contains significant amounts of Na. To explain these findings, it was suggested that Na addition to Al_2O_3-SiO_2 glasses suppresses the population of tetrahedral

triclusters and as a consequence the difference in the short range orders of mullite and the aluminium silicate melt becomes greater and therefore the nucleation barrier for mullite formation in Na_2O-Al_2O_3-SiO_2-melts is higher than in Al_2O_3-SiO_2 melts. Since mullite crystallization in the bulk of the liquid phase becomes unfavorable if Na is present, growth of mullite needles from the surface of the single crystal substrate occurs instead.

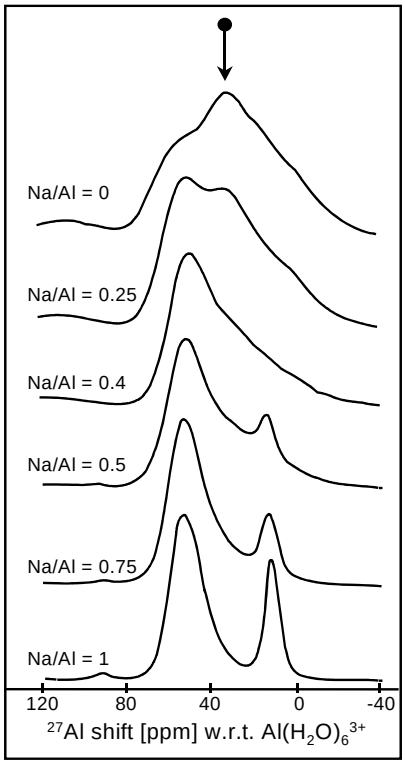

Fig. 14: ^{27}Al MAS NMR spectra of aluminium silicate glasses containing 10 mol% Al_2O_3 and varying amounts of Na_2O. Note the decreasing intensity of the 30 ppm resonance (arrow) with increasing Na content ***(from Schmücker et al., 1997)****.*

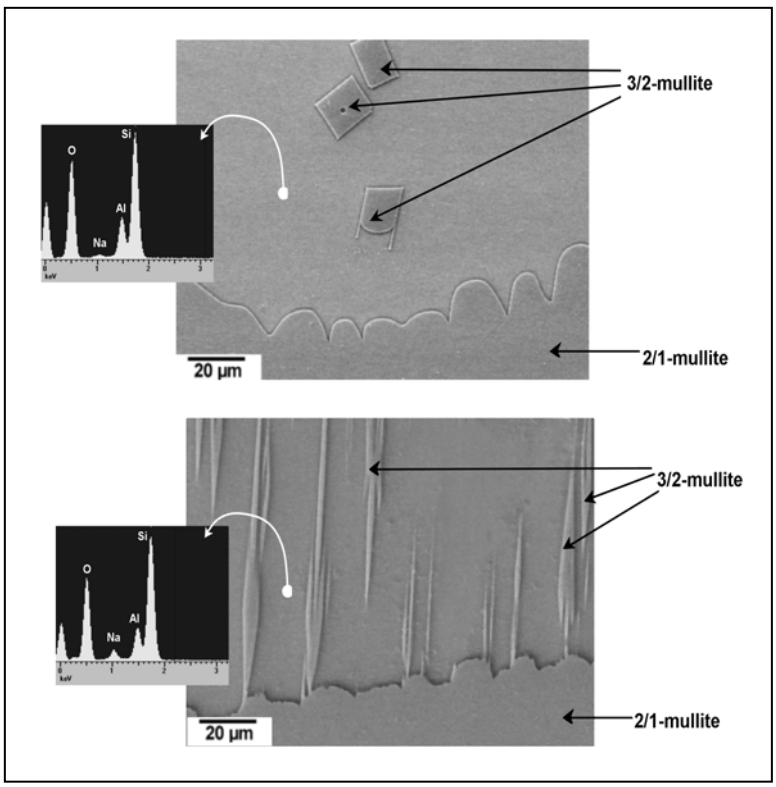

Fig. 15: Cross section micrograph of mullite single crystal /SiO_2-Al_2O_3 glass (a) and mullite single crystal / SiO_2-Na_2O-Al_2O_3 glass (b) heat-treated for 100 h at 1650 °C: Newly formed mullite crystallites appear in the bulk of the pure aluminium silicate glass (a) but grow epitactically from the substrate surface into the sodium silicate melt (b). Inserts: EDX spectra of the vitreous phases (from ***Schmücker and Schneider, 2002a****).*

Metastable immiscibility

Demixing occuring in non-crystalline materials of the system SiO_2-Al_2O_3 has been well established for many years. MacDowell and Beall (1969) were among the first reporting the existence of a metastable immiscibility region which was deduced from microstructural investigations of rapidly quenched aluminium silicate glasses. Fig. 16 shows the microstructure of a rapidly solidified aluminium silicate glass with mullite composition. The as-quenched glass appears featureless (Fig. 16a) while annealing at 890 °C produces significant segregation effects (Fig. 16 b).

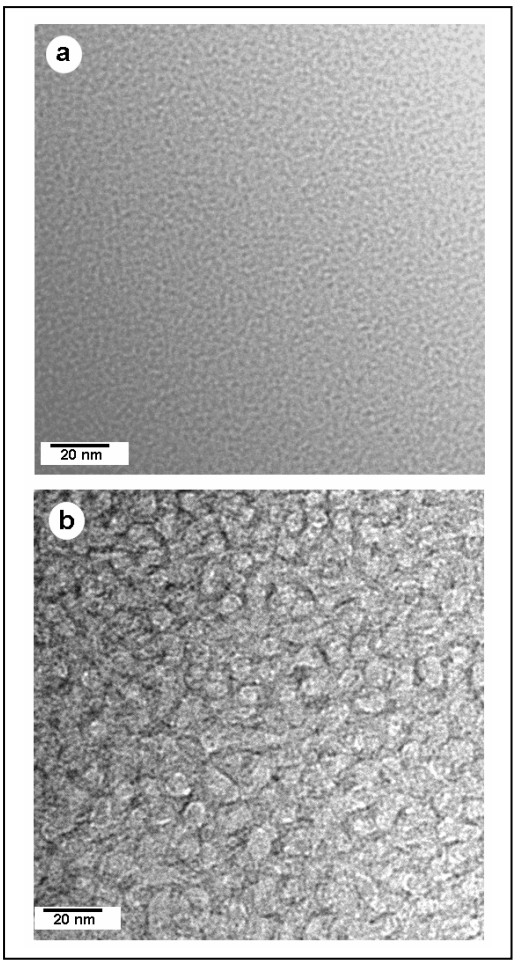

Fig 16: TEM micrograph of rapidly quenched aluminium silicate glass (a). After calcination below crystallization temperature (890 °C) demixing zones become visible (b), ***(Schmücker, unpublished)***

Ban et al. (1996) emphasized that mullite crystals formed in glasses and ultrahomogeneous gels at T < 1000 °C are considerably supersaturated in Al_2O_3 irrespective of the bulk chemical composition of the starting material. It was assumed that the unusual crystallization behaviour of mullite is caused by phase separation in the amorphous state and that the composition of mullite formed at, say 950 °C, corresponds to the alumina-rich demixing zones existing at this temperature. Rapid mullite crystallization at temperatures above ≈950 °C, however, disturbs the observation of metastable phase separation and hence it is extremely difficult to determine the high temperature region of the immiscibility gap by experimental methods. There have been several approaches for

calculating the immiscibility region from thermodynamic data. Risbud and Pask (1977) calculated the immiscibility gap for the pseudobinary system SiO_2-mullite using a regular solution model. Ban et al. (1996) also assumed a regular solution model but considered the binary system SiO_2-Al_2O_3. Takei et al. (2000), on the other hand, used thermodynamic parameters derived from molecular dynamics simulations. The calculated immiscibility regions are plotted in Fig. 17 together with typical compositions of mullite formed at 950 °C and 700 °C (**Fischer et al. 1994**), respectively. The immiscibility gap calculated by Ban et al. fits well with the crystallization temperature/composition data determined for mullite. However, the extension of the immiscibility gap towards SiO_2 may correspond to Risbud´s or Takei´s calculations rather than to Ban´s curve since no phase separation could be observed in silica glasses with 5 mol% Al_2O_3 prior to mullitization (**Schmücker, unpublished results**).

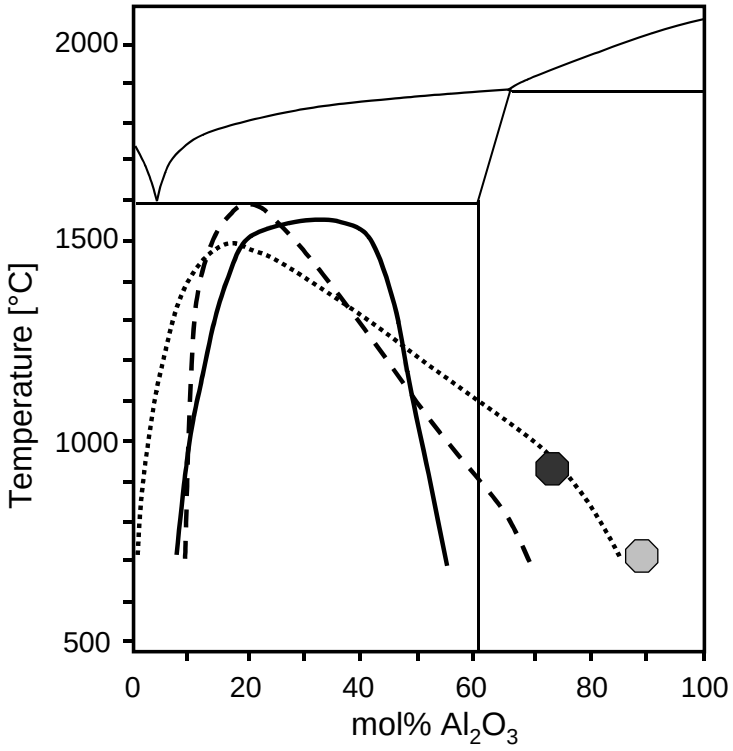

*Fig. 17 : Metastable immiscibility in the system SiO_2-Al_2O_3 after Risbud and Pask, 1977 (full line), Ban et al., 1996 (dotted line), and Takei et al., 2000 (dashed line). Data points correspond to mullite compositions formed at 980 °C and 700 °C (**Fischer et al., 1994**), respectively.*

2.3. Crystallization of type I mullite precursors

Crystallization studies on ultrahomogeneous mullite gels and related glasses were performed by isothermal and dynamic XRD experiments (Takei et al. 1999, Li and Thomson, 1990), isothermal DSC (Tkalcec et al., 1998, Johnson et al., 2001) and non-isothermal DTA (Takei et al., 2001), all combined with electron microscopical investigations. The following conclusions can be drawn from the literature data:

- Mullite is formed at T<1000 °C in the bulk of its non-crystalline precursor.
- The nucleation density of mullite is extremely high (≈10^{17} cm^{-3}, see also Fig. 10) and crystal growth is a three-dimensional process.
- Kinetic analyses show that the transformation process is a two step reaction. This finding is generally explained by phase separation in the non-crystalline material prior to crystallization (see above). Evidence suggests that the mullitization temperature is slightly lower in the alumina-rich domains than in the alumina-poor domains.

Aside from the data published by Li and Thomson, activation energies of mullite crystallization range between 850 and 1300 kJ/mol. The former authors, however, determined activation energies of mullite formation as low as 300-400 kJ/mol. Mullite nucleation is another point of controversy. According to Li and Thomson mullite crystallization starts without an induction time at temperatures as low as 940 °C. Takei et al. (1999), on the other hand, observed a distinct nucleation period characterized by an increasing number of newly-formed mullite crystallites of constant size. The time/temperature correlation of the incubation time τ was used to estimate the activation energy of nucleation (980 kJ/mol) which is somewhat smaller than the activation energy determined for subsequent crystal growth (≈1100 kJ/mol). Johnson et al. stated that aluminium silicate glass samples are fully nucleated by the time they reach 850 °C and hence crystallization occurs with a constant number of nuclei. James et al. (1997), on the other hand, reviewing the nucleation rates of various silicate glasses, found that maximum nucleation temperature (T_M) is strongly correlated to the liquidus temperature (T_L), thus leading to T_M/T_L ratios scattering in a remarkably narrow range of 0.54 to 0.58. Using these data, the T_M of mullite glasses is between 895 and 980 °C suggesting that the formation of mullite at temperatures above 900 °C is not only due to the growth of pre-existing nuclei but comprises both, nucleation and growth. Inconsistencies in Johnson´s findings may be due to the fact that the aluminium silicate glasses of the latter were prepared with moderate quenching rates (≈250 °C/s) and hence mullite nucleation may have occurred during the cooling period.

3. Precursors transforming to mullite above 1200 °C by alumina-silica reaction (Type II)

Ultrahomogeneous mullite precursors allow mullitization below 1000 °C (see 2.3.). However, once mullite is formed, densification of the resulting ceramic is difficult as diffusional processes in mullite are sluggish. Since mullitization and densification are obviously two competitive mechanisms, retarded mullite formation from highly dispersed Al_2O_3 / vitreous silica admixtures allows significant densification prior to mullitization by a viscous sintering mechanism. Thus, true diphasic mullite precursors (type II precursors, Schneider et al., 1993b) are most important from a technological

point of view. Diphasic mullite precursors with constituents ranging from a few to several hundreds of nanometers are prepared predominantly by sol-gel- or precipitation techniques, though well homogenized ground powders of alumina and silica phases may also come into that category.

3.1 Preparation of diphasic (type II) mullite precursors

Preparation of diphasic mullite precursors by sol-gel methods originates from the pioneering work of Hoffman et al. (1984). In their studies diphasic mullite precursors were synthesized using aqueous silica sol and boehmite sol as starting materials. Gelation was carried out by gradual solvent evaporation. In alternative approaches admixtures of a sol and a true solution (boehmite sol plus alcoholic tetraethoxysilane -TEOS- solutions or silica sol plus aqueous aluminium nitrate solution, respectively) have been employed. Okada and Otsuka (1986) used demixed alcoholic solutions of TEOS plus aluminium chloride and gelled them after slow hydrolysis. More recently, Voll (1995) prepared diphasic mullite precursors starting with alcoholic solutions of TEOS and Al-sec-butylate. TEOS solution was prehydrolised by addition of water under strongly basic conditions (pH = 13) to induce SiO_2 self condensation. After a short aging time the silica sol containing considerable amounts of excess water was put into the Al-bearing solution immediately leading to hydrolysis of Al-sec-butylate and subsequent formation of pseudo-boehmite colloids. TEM investigation of the dried gel reveals the existence of relatively large spherical SiO_2 particles and nanometer-sized pseudo-boehmite aggregates the latter intimately embedded in a non-crystalline SiO_2 matrix (Fig. 18).

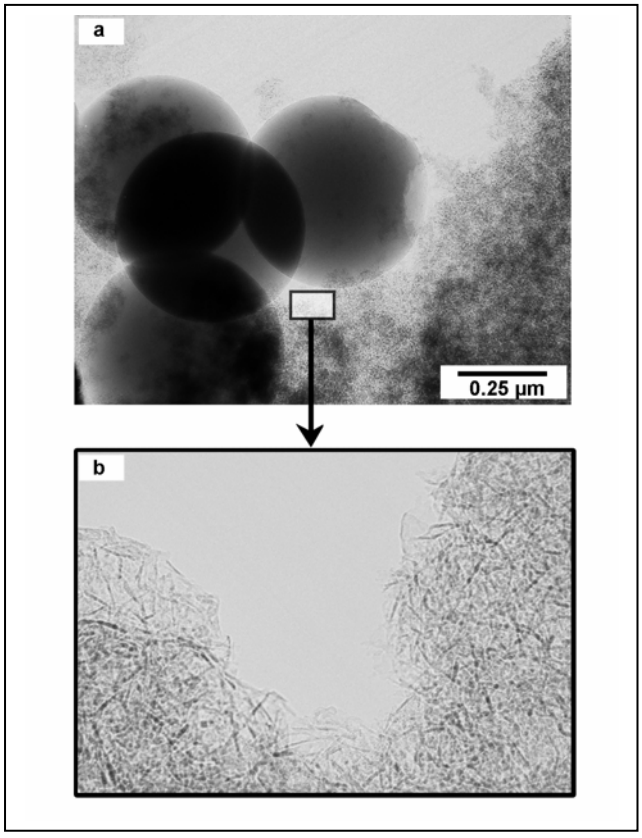

Fig. 18: Diphasic mullite precursor consisting of relatively large spherical SiO_2 particles and nanometer-sized pseudo-boehmite aggregates intimately embedded in a non-crystalline SiO_2 matrix (TEM). a: Overview, b: Detail of pseudo-boehmite aggregate, ***(Schmücker, unpublished)***

A novel preparation method for diphasic mullite precursors was proposed by Sacks et al., (1991). According to this concept the powder particles of the mullite precursor are "microcomposites" consisting of an α-Al_2O_3 core surrounded by amorphous silica. Al_2O_3/SiO_2 microcomposites were prepared by dispersing the fractionated (≈0.2 µm) alumina particles in an alcoholic TEOS solution. Subsequent silica precipitation at the surface of the alumina particles was induced by the addition of ammoniated water. Compacts of the composite particles sintered to almost full density at ≈1300 °C by viscous deformation of the amorphous silica layer (transient viscous flow sintering "TVS"). On the other hand, the relatively long diffusion distances (≈200 nm) require rather high mullitization temperatures (≈1500 °C). Based on the idea of microcomposite powders, **Bartsch et al. (1998)** prepared "nanocomposite" mullite precursors consisting of γ-alumina particles coated by a nanometer silica layer (Fig. 19). Compacts of γ-Al_2O_3/SiO_2-nanocomposites exhibit a similar densification behaviour by TVS as corresponding α-Al_2O_3/SiO_2-microcomposites but mullite forms at a significantly lower temperature (≈1300 °C) since the diffusional distances required for mullitization are about one order of magnitude smaller.

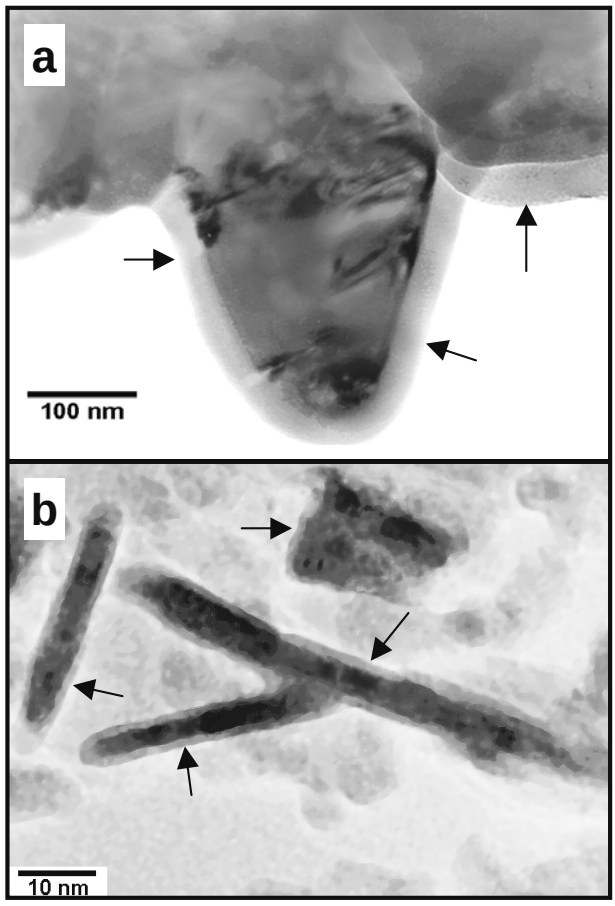

*Fig. 19: Diphasic mullite precursor prepared by coating of α-Al_2O_3 powder (a) and γ-Al_2O_3 powder (b) with amorphous silica (arrows), from **Bartsch et al., 1998**.*

3.2 Transformation behaviour of diphasic mullite precursors

The transformation of diphasic mullite precursors consists of two steps:

- Development of transition alumina phases below ≈1200 °C
- Mullite formation by reaction of alumina polymorphs with silica polymorphs above 1200 °C.

Composition of the spinel-type transition alumina phase

Diphasic mullite precursors prepared by sol-gel methods typically consist of pseudoboehmite (γ-AlOOH) plus amorphous silica (e.g Hoffman et al., 1984). By dehydration above ≈500 °C pseudoboehmite converts to spinel-type γ-Al_2O_3 the latter then transforms into structurally related δ- and θ -Al_2O_3 (Wefers and Misra, 1987). The composition of the spinel-type transition alumina phases have been a point of controversy for many years: The spinel type transition phase occurring during the kaolinite-mullite transformation was found to incorporate considerable amounts of Si. This was derived from leaching experiments and analytical TEM investigations that revealed (Al,Si)-spinel compositions approaching mullite composition (e.g. Chakraborty and Gosh, 1978, Srikrishna et al., 1990). Brown et al. (1985) on the other hand, using ^{29}Si NMR spectroscopy established virtually Si-free γ-Al_2O_3 as the transient phase in the kaolinite-mullite reaction sequence. Contradictory results have also been reported for the spinel-type transient phase occurring in gel-derived mullite precursors: Low and McPherson (1989), based on IR spectroscopic investigations, assumed a composition corresponding to that of 2/1-mullite, while Wei and Halloran (1988a) and Komarneni and Roy (1986) deduced by ATEM microanalysis and Si-NMR spectroscopy, respectively, that the spinel phase is essentially pure aluminium oxide. Okada and Otsuka (1986) compared the IR spectrum of pure γ-Al_2O_3 with that of the mullite gel derived spinel phase and concluded significant Si incorporation for the latter. By means of ATEM the Al_2O_3/SiO_2 ratio of the (Al,Si) spinel was determined to be 6/1.

Schneider et al. (1994c) reexamined the composition of the transient spinel phase that develops in TEOS plus Al-sec-butylate-derived mullite precursors (see above) by combining spectroscopic methods (IR, ^{27}Al-NMR, ^{29}Si-NMR) with analytical TEM on leached and non-leached samples all calcined between 350 and 1150 °C. The dried precursor powder consists of relatively large spherical SiO_2 particles and much finer grained agglomerates of pseudo-boehmite embedded in a SiO_2 matrix (Fig. 18). Above ≈350 °C the pseudo-boehmite/silica admixture converts completely to (Si,Al) spinel with ≈12 mol% SiO_2. Up to 750 °C the composition of the spinel phase remains constant, but above this temperature the SiO_2 content gradually increases up to ≈18 mol% at 1150 °C (Fig. 20), obviously by partial dissolution of the larger SiO_2 spherules.

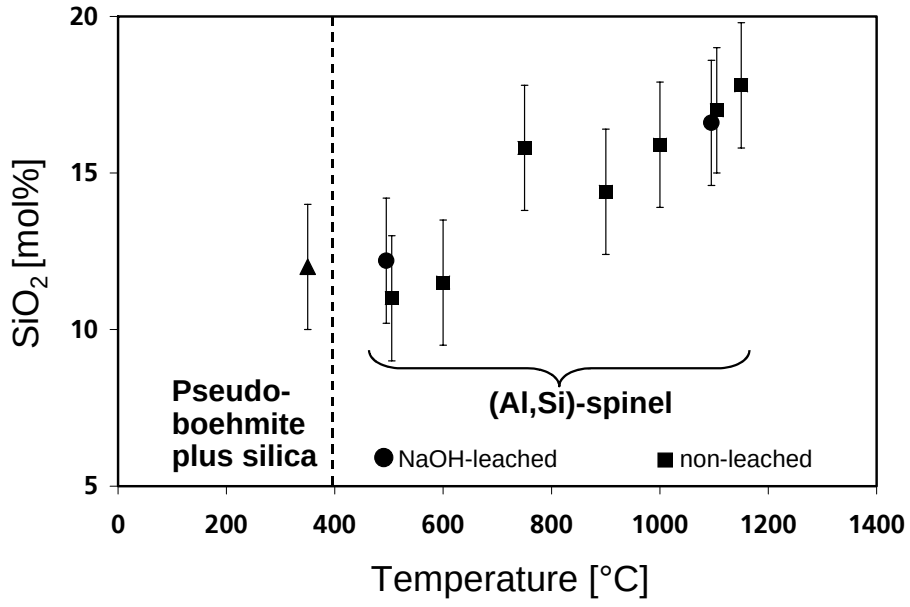

Fig. 20: SiO_2 content of pseudo-boehmite plus silica phase assemblage and of spinel-type transition alumina determined by TEM-EDX. As leaching of the spinel phase has no influence on the determined composition, it is concluded that SiO_2 has incorporated the spinel phase, after ***Schneider et al., 1994****.*

Mullite formation

Wei and Halloran (1988a,b) were among the first to study the transformation behaviour of diphasic mullite precursors and mullite formation kinetics. The diphasic starting materials were obtained by admixing a prehydrolized TEOS solution with a pseudo-boehmite sol. Mullite was considered to form by direct solid-state reaction between the transition alumina phase and the silica-rich non-crystalline phase by a process either interface-controlled or short range diffusion-controlled. Quantitative X-ray diffraction data revealed that mullite formation is preceded by an incubation period that includes diffusion and reaction processes to form mullite nuclei. The apparent activation energy of mullite incubation is 987±63 kJ/mol which is close to the activation energy of the overall transformation process (1070±200 kJ/mol). Based on SEM analyses the nucleation density of diphasic mullite gels has been calculated to be $\approx 2 \times 10^{11}/cm^3$ which is significantly smaller than nuclei densities derived from single phase gels ($\approx 10^{17}$ cm^{-3}, see Fig. 10). Analyses of average mullite grain sizes as a function of calcination time revealed a time-dependent growth rate proportional to $t^{-0.63}$.

Transformation of diphasic mullite precursors with various bulk compositions was investigated by Li and Thomson (1991) using differential thermal analysis. Reported activation energies scatter around 1000 kJ/mol. Similar values (1034±124 kJ/mol) were determined by Huling and Messing (1991). A somewhat smaller activation energy of mullite formation (880±30 kJ/mol) was established by Boccaccini et al. (1999). Their diphasic mullite precursor was prepared by admixing nanometer-sized fumed silica (aerosil) with boehmite sol and was subsequently gelled. The slightly

lower activation energy with respect to the above-mentioned data was attributed to the different starting materials i. e. fumed silica as Si source instead of hydrolized TEOS solutions. **Hildmann et al. (1996)** investigated mullite formation in nanomter-sized phase assemblages of transition alumina plus non-crystalline silica, the latter containing 2 wt. % B_2O_3. The apparent activation energy of the mullite incubation period, as derived from quantitative X-ray data, was ≈650 kJ/mol while the activation energy of the overall transformation process was 900 kJ/mol. The latter corresponds reasonably to the values given above, but the activation energy of the incubation time is significantly lower than corresponding data for B_2O_3-free materials. Data suggest that the nucleation barrier of mullite is clearly lowered by the B_2O_3-addition which is supported by the observation of much higher nucleation density (≈10^{15} /cm^3) with respect to diphasic pure mullite precursors.

Sundaresan and Aksay (1991) reexamined the kinetic data given by Wei and Halloran. It was emphasized that the reported time-dependent growth rate is not consistent with an interface-controlled or short range diffusion-controlled transformation mechanism but is in excellent accordance with a dissolution/precipitation mechanism. In this scenario the alumina particles dissolve into the silica phase and mullite nuclei form when the vitreous aluminium silicate phase exceeds a critical concentration. The solution/precipitation process can be illustrated by a schematic free enthalpy vs. composition diagram (Fig. 21). Construction of common tangents reveals that the equilibrium composition of the amorphous phase is richer in Al_2O_3 when coexisting with alumina (SA) than when coexisting with mullite (SM). Thus, the amorphous phase is able to incorporate Al_2O_3 up to SA as long as no mullite exists. On the other hand, mullite nucleation may occur if the critical nucleation concentration (CNC) is reached at some point to the right of SM.

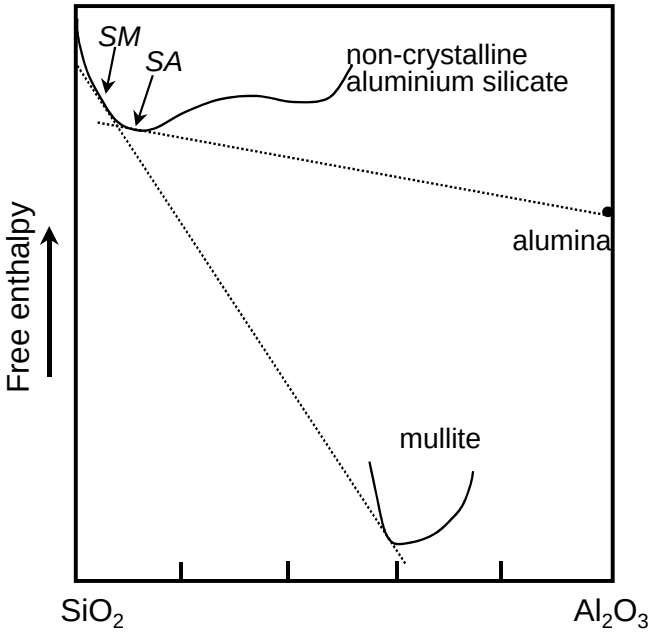

Fig. 21: Schematic free enthalpy diagram of the system SiO_2-Al_2O_3 (after Sundareasan and Aksay, 1991). SM and SA are the compositions of the non-crystalline aluminium silicate phase coexisting with mullite and alumina, respectively.

According to Sundaresan and Aksay, mullite nucleation within the non-crystalline silica-rich phase implies that dissolution of alumina is the rate-controlling step in mullite growth. Diffusion of Al ions through the vitreous phase as the rate-controlling step was ruled out, since in that case a compositional gradient has to be expected within the silica-rich phase giving rise to mullite formation at the Al_2O_3/SiO_2 interface rather than in the bulk of the silica-rich phase. Mullite as interfacial product, however, has been reported to occur using sapphire/SiO_2 reaction couples heated at temperatures above 1678 °C (Aksay and Pask, 1975). Thus, a change of the rate-limiting effects at some point between 1350 °C and 1650 °C was postulated by Sundaresan and Aksay, whereby dissolution is thought to be rate-controlling below and diffusion is rate-controlling above this temperature.

Microscopic evidence for the solution/precipitation mechanism and for the crossover behaviour between dissolution- and diffusion-controlled mullite formation was provided for the first time by **Schmücker et al. (1994)** investigating the mullitization of α- Al_2O_3/quartz powder admixtures. The starting powders used in this study were relatively coarse (>100 nm) compared with the alumina and silica particles occurring in gel-derived mullite precursors and hence elevated mullitization temperatures of ≈1500 °C were required. Since quartz grains form a (metastable) viscous melt layer at their peripheries upon (rapid) heating at temperatures >1300 °C, the investigated mullitization reaction takes place between Al_2O_3 and amorphous SiO_2 rather than between Al_2O_3 and quartz (Fig. 22a). Upon heating the powder admixtures to 1550 °C, mullite crystallites which are randomly nucleated within the non-crystalline silica-rich phase were detected (Fig. 22b).

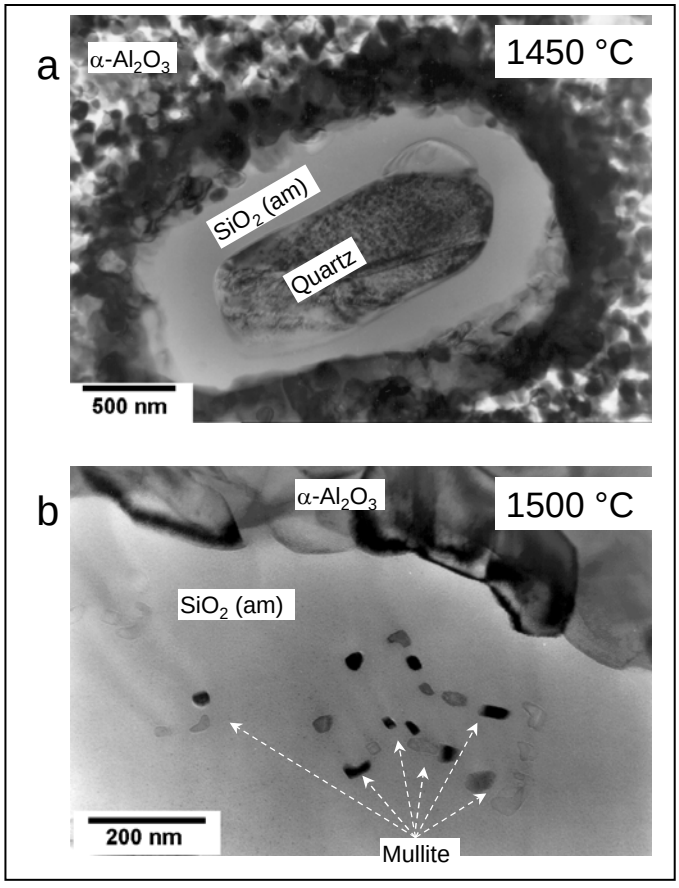

Fig. 22: Quartz/α-Al_2O_3 powder admixtures sintered at 1450 °C and 1500 °C, respectively. Upon heating at 1450 °C, quartz grains form a (metastable) viscous melt layer at their peripheries (a). Firing at 1500 °C leads to formation of randomly oriented mullite crystallites within the liquid siliceous phase (b), from ***Schmücker et al., 1994****.*

The compositional development of the vitreous phase determined by numerous EDX-analyses is shown in Fig. 23. Analytical data show that ≈4 mol% Al_2O_3 is incorporated into the viscous silica melt at temperatures of 1450 and 1475 °C. Firing temperatures of 1500 °C, on the other hand, lead to a bimodal compositional distribution with maxima at ≈4 and ≈2.5 mol% Al_2O_3. The obvious reduction of the Al_2O_3 content is attributed to mullite crystallization in the non-crystalline aluminium silicate phase occurring at this temperature. Evidence suggests that the composition of the silica-rich melt coexisting with mullite (SM) is ≈97.5 mol% SiO_2, ≈2.5 mol% Al_2O_3 while the critical concentration of mullite nucleation (CNC) is ≈4 mol% Al_2O_3 at 1550 °C (Fig. 24).

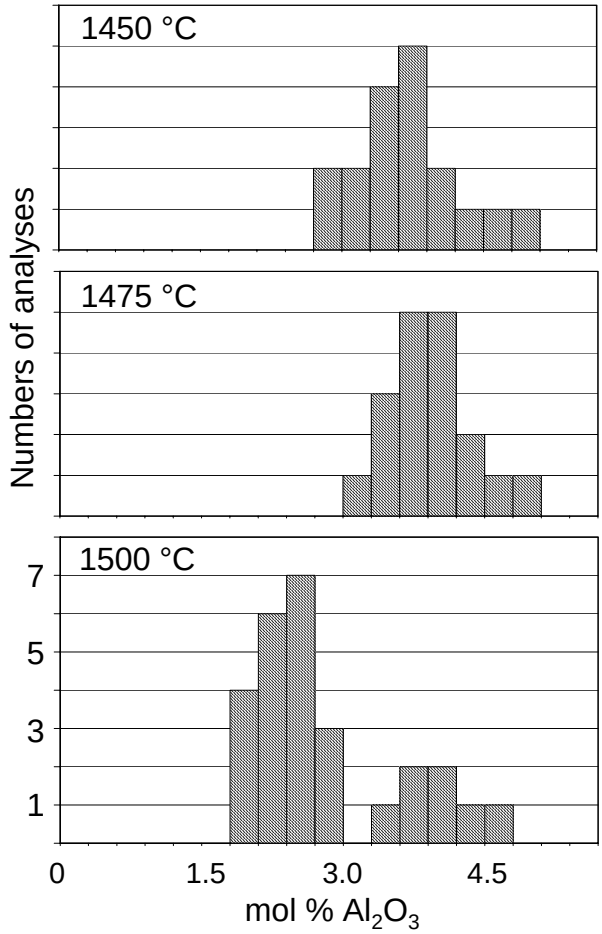

*Fig. 23: Composition of the siliceous melt formed at the periphery of quartz grains during reaction sintering (see Fig. 22). The silica-rich melt incorporates ≈4 mol% Al_2O_3 prior to mullite nucleation. After mullite nucleation (1500 °C) the alumina content of the liquid phase is ≈2.5 mol% Al_2O_3 (from **Schmücker et al., 1994**).*

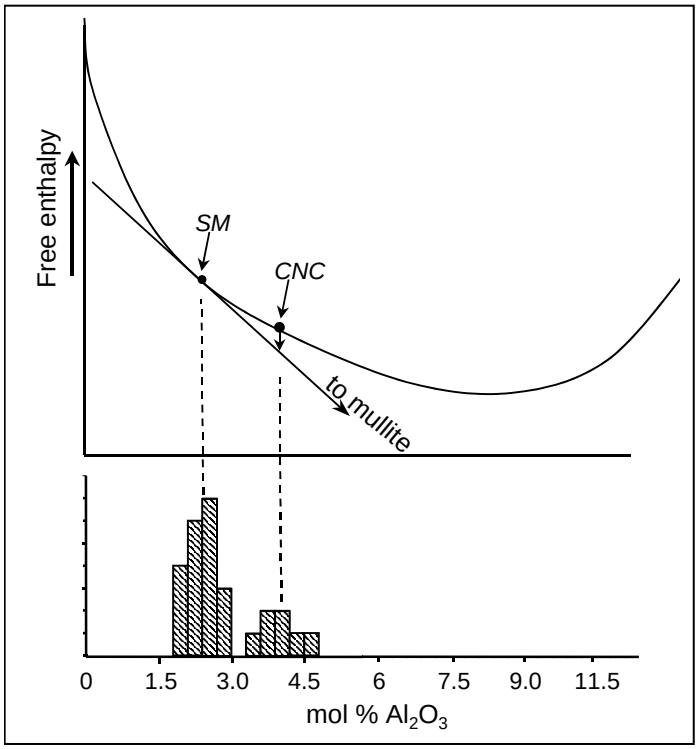

Fig. 24: Bimodal compositional distribution of the siliceous phase occurring during reaction sintering of quartz plus α-Al_2O_3 (see Figs. 22 and 23) suggests that SM (i.e. the composition of the silicate melt coexisting with mullite, see Fig. 21) is ≈2.5 mol% Al_2O_3, while the critical nucleation concentration (CNC) is ≈4 mol% Al_2O_3.

The microstructure of quartz/alumina powder admixtures heat-treated at 1600 °C provides evidence for a change in the mullite formation mechanism. Though silica has converted completely to cristobalite, the extension of previous outer melt zones can be recognized by orientational

contrasts of the cristobalite. It is noteworthy that no mullite crystals are incorporated in the outer cristobalite zone, but a mullite layer forms at the α-Al_2O_3/SiO_2 contact instead (Fig. 25). Mullite formation close to the Al_2O_3/SiO_2 interface is consistent with the model of Sundaresan and Aksay suggesting diffusion-controlled mullite growth at high temperatures. Thus, these experimental data imply that temperatures of 1550-1600 °C correspond to the predicted crossover temperature between dissolution-controlled and diffusion-controlled mullitization.

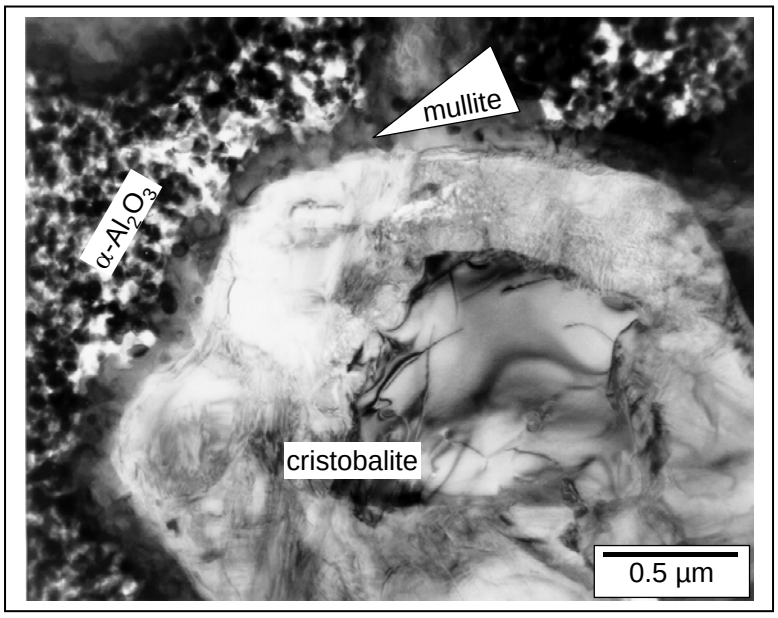

*Fig. 25: Microstructure of quartz/ α-Al_2O_3 powder admixtures sintered at 1600 °C signals a different reaction mechanism with respect to firing conditions of 1500 °C: No mullite crystals are incorporated in the peripheral SiO_2 zone, but a mullite layer forms at the α-Al_2O_3/SiO_2 contact instead (from **Schmücker et al., 1994**).*

Recently Kleebe et al. (2001), when investigating mullitization in α-Al_2O_3/SiO_2 powder admixtures, found evidence for the dissolution/precipitation mechanism if 300 nm α-Al_2O_3 particles are used. In contrast, if Al_2O_3 particles of 2 µm were employed, intense alumina-enrichment of the vitreous phase at the Al_2O_3/SiO_2 interface occurs, subsequently leading to a thin interfacial mullite zone. The grain-size-induced change in crystallization mechanism obviously cannot be explained in terms of a transition between dissolution and diffusion-controlled mullitization, since dissolution as the rate-limiting step (and hence mullite formation within the bulk of the siliceous phase) is expected for larger alumina grains rather than for smaller ones. Kleebe et al. argued that in case of the micron-sized alumina starting powder accelerated cristobalite formation gives rise to alumina enrichment in the peripheral zone of the siliceous phase and subsequently to mullite formation.

4. Type III mullite precursors and precursors ranging between ultrahomogeneous and diphasic

Ultrahomogeneous (type I) mullite precursors are non-crystalline and convert directly to Al_2O_3-rich mullite at ≈950°C (ch. 2). Diphasic precursors (type II) typically consist of a poorly crystalline aluminium (hydr)oxide plus non-crystalline silica reacting to mullite above 1200 °C (ch. 3). A further non-crystalline mullite precursor type, however, has been described in literature designated as rapid hydrolysis gel (Okada and Otsuka, 1986) or type III gel (Schneider et al., 1993a). The crystallization temperature of type III aluminium silicate gels corresponds to type I mullite precursors but spinel-type transition alumina is the first crystalline phase while mullite forms by Al_2O_3/SiO_2 reaction at ≈1200 °C in the same way as in diphasic precursors. Previous studies reveal that a gradual transition may exist between type I and type III precursors, resulting in predominantly mullite, mullite plus γ-Al_2O_3, or predominantly γ-Al_2O_3 crystallization (Voll, 1995, Taake, 1999, see also Fig. 26).

Type III gels: Preparation and structural investigations

Preparation of type III gels by various routes has been reported. Okada and Otsuka (1986) and Hyatt and Bansal (1990) used TEOS ($Si(OC_2H_5)_4$ and $Al(NO_3)_3{\cdot}9H_2O$-solutions as starting compounds, and gelled the solutions after rapid hydrolysis at 60 °C. Slow hydrolysis of TEOS plus $Al(NO_3)_3{\cdot}9H_2O$-solutions at 60 °C was reported to produce ultrahomogeneous (type I) mullite precursors (see above), but type III gels can be achieved by slow hydrolysis if the sol is aged at room temperature instead of 60 °C (Okada et al, 1996, Taake, 1999). It was shown that the mullite gels gradually change from type III to type I on increasing the aging temperature from 20 to 60 °C (Fig. 26). Voll (1995) prepared diphasic mullite precursors starting with alcoholic solutions of TEOS and Al-sec-butylate by a similar method as described for the preparation of diphasic gels. The TEOS solution was prehydrolised but mild basic conditions (pH 7-10) were used to prevent SiO_2 - self condensation.

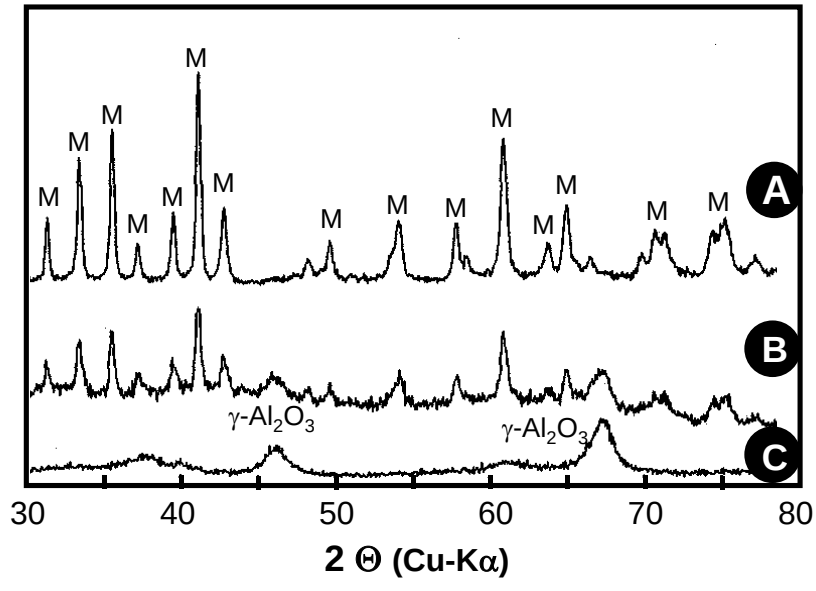

*Fig. 26: Mullite precursors prepared from TEOS ($Si(OC_2H_5)_4$ and $Al(NO_3)_3{\cdot}9H_2O$-solutions gelled at 60 °C (A), 40 °C (B), and 20 °C (C), respectively, after firing at 1000 °C. If low gelation temperatures were used, the precursor converts into transition alumina (plus amorphous silica) rather than into mullite (**unpublished data**).*

Different crystallization behaviour of type I and type III gels was generally explained by less intimate cation mixing of the latter, thus leading to γ-Al_2O_3 crystallization rather than to direct mullite formation (e.g. Schneider et al., 1994b, Okada et al., 1996). Schneider et al. (1993b), on the other hand, pointed out that ^{29}Si NMR spectra of type I and type III gels are fairly similar which is not consistent with significant demixing in type III mullite precursor. ^{27}Al NMR spectroscopy, however, provided evidence for higher amounts of AlO_6 polyhedra in type III gels than in type I gels and it was argued that sixfold coordinated Al may facilitate formation of spinel-type transition alumina phases (Schneider et al., 1993b).

The structural development of TEOS plus $Al(NO_3)_3 \cdot 9H_2O$ derived type III gels synthesized by aging at room temperature was recently investigated by **Schmücker and Hoffbauer** (unpublished results). By means of ^{29}Si NMR spectroscopy gel powders calcined between 900 and 1200 °C were investigated in order to cover the whole transformation range (Fig. 27). Gels calcined at 900 °C show a single resonance centering at ≈90 ppm being typical for tetrahedrally coordinated Si in aluminium silicates (mullite, aluminium silicate glasses, ultrahomogeneous gels, see ch. 2.2). Obviously Si environments of type I and type III gels are very similar. Moreover, phase separation assumed to occur in the amorphous state just prior to crystallization, can be ruled out. Between 950 and 1100 °C a signal centered at 110 ppm is observed with a shoulder in the 90 ppm region. The corresponding Si sites are attributed to spinel-type transient phase with minor Si incorporation (90 ppm) and to the coexisting vitreous silica. Above 1100 °C the spinel phase and silica gradually react to form mullite monitored by a gradual increase of the 90 ppm resonance.

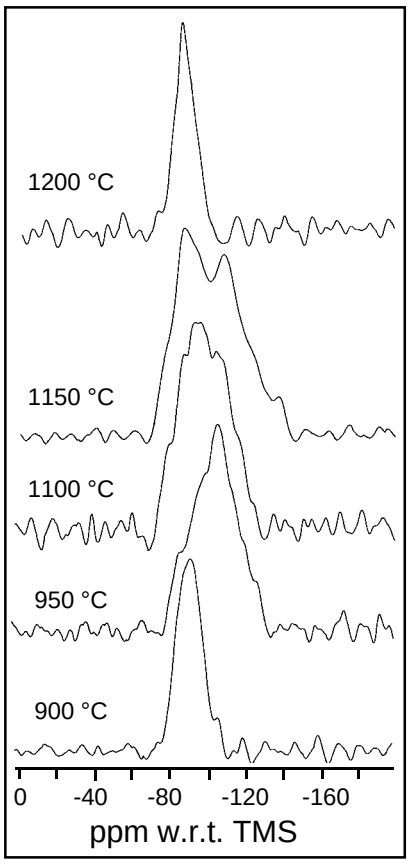

Fig. 27: ^{29}Si NMR spectra of type III mullite gels heat-treated between 900 and 1200 °C. Gels calcined at 900 °C (amorphous) and 1200 °C (after mullite formation) show a single resonance centered at ≈90 ppm typical of tetrahedrally coordinated Si in aluminium silicates. Between 950 and 1100 °C a signal centered at 110 ppm is observed with a shoulder in the 90 ppm region. The corresponding Si sites are attributed to spinel-type transient phase with minor Si incorporation (90 ppm) and to the coexisting vitreous silica (110 ppm).
*(**Schmücker and Hoffbauer**, unpublished)*

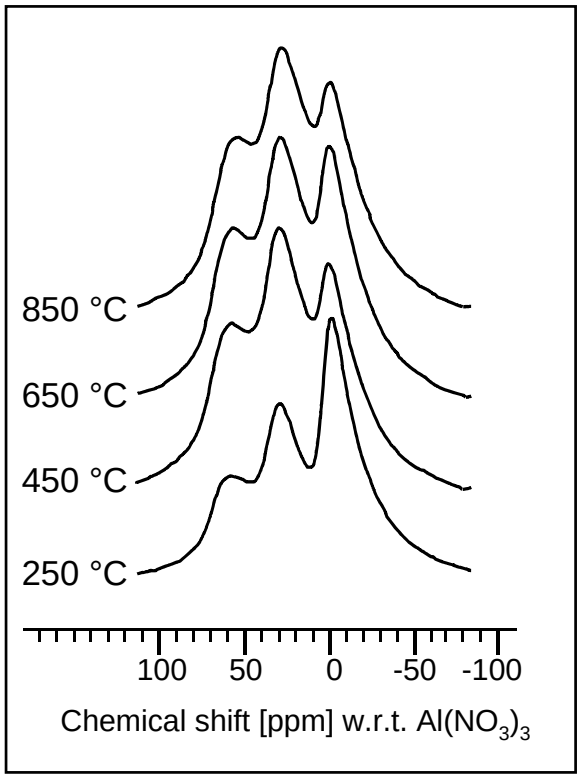

Fig. 28: ^{27}Al NMR spectra of type III mullite gels heat-treated at different temperatures prior to crystallization. The structural development corresponds to type I gels (Fig. 9).
***Schmücker and Hoffbauer**, unpublished*

^{27}Al NMR spectra of type III gels in the non-crystalline stage (150 °C - 900 °C) are shown in Fig. 28. It becomes obvious that the spectral development is virtually the same as observed in ultrahomogeneous typ I gels (see Fig. 9). NMR data reveal that there is no significant structural difference between non-crystalline type I and type III gels. Subtle differences in compositional homogeneity may exist, but experimental evidence is hard to obtain.

Limits between ultrahomogeneous and diphasic mullite precursors

To shed light on the field between ultrahomogeneous and diphasic mullite precursors and to provide a correlation between possible demixing effects in non-crystalline aluminiumsilicates and related crystallization behaviour **Schmücker et al. (2001)** prepared noncrystalline aluminium silicate material having a priori well-defined degrees of chemical inhomogeneity ranging from a nanometer to almost atomic scale. For that purpose aluminosilicate films consisting of thin (≈30 nm) to ultrathin (≈2 nm) Al_2O_3 and SiO_2 sublayers were vapour deposited by two source evaporation using a jumping beam technique (EB-PVD). Four series of PVD films were produced under variation of jumping beam frequencies. All films were non-crystalline with chemical bulk compositions ranging between 50 and 63 mol% Al_2O_3. Film thickness, deposition rates, jumping beam frequencies and nominal thickness of periodical Al_2O_3/SiO_2 sequences are summarized in Table 2.

	Series 1	Series 2	Series 3	Series 4
Film thickness	70 µm	75 µm	30 µm	29 µm
Average Deposition rate	190 nm/s	125 nm/s	75 nm/s	50 nm/s
Jumping beam frequency	7 Hz	14 Hz	14 Hz	25 Hz
Nominal thickness of Al_2O_3-SiO_2 double layer	27 nm	9 nm	5.5 nm	2 nm

*Table 2: Experimental conditions of electron beam physical vapour deposition (EB-PVD) runs (**Schmücker et al., 2001**)*

TEM cross sections of the PVD films reveal a sequence of periodic contrasts occurring perpendicular to the deposition direction. The contrast periodicities correspond reasonably with the calculated thicknesses of the respective Al_2O_3/SiO_2 double layers. EDX line scans confirm that the alumino silicate PVD films consist of Al_2O_2- and SiO_2-rich sublayers (Fig. 29).

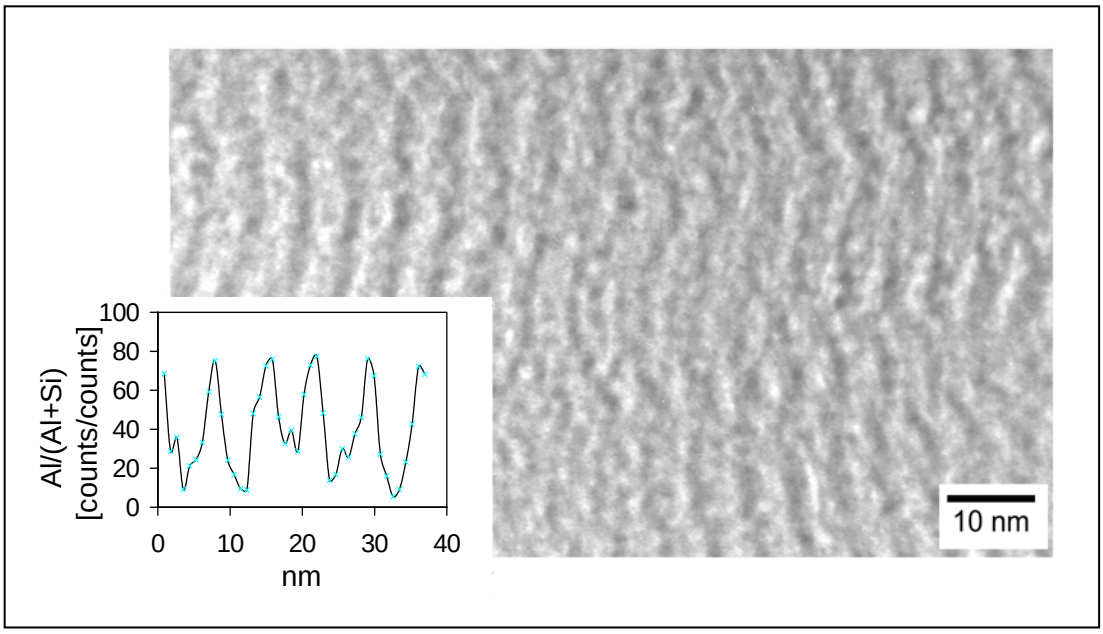

*Fig. 29: Cross section transmission electron micrographs of physical vapor deposited alumino silicate double layers (series 2) in high magnification with EDX-line scan perpendicular to the observed contrast modulations. EDX profile yields evidence for periodical chemical variations (from **Schmücker et al., 2001**).*

^{29}Si NMR spectra obtained from series 1 (≈30nm SiO_2/Al_2O_3-double layer thickness), series 3 (≈5nm SiO_2/Al_2O_3-double layer thickness), and series 4 (≈2nm SiO_2/Al_2O_3-double layer thickness) are shown in Fig. 30: All spectra are very similar and exhibit a resonance in the 110 ppm region. The peak profiles, however, are slightly asymmetric indicating a resonance of minor intensity in the 90 ppm region. Deconvolution of the asymmetric resonances into 2 signals centering at ≈110 and

at ≈90 ppm, respectively, results in a peak area ratio of ≈9/1. This means that virtually pure SiO_2 layers (110 ppm resonance) occur in all EB-PVD aluminosilicate films investigated. The minor fraction of Si sites surrounded by Al (90 ppm resonance) is interpreted in terms of interfacial Si sites, taking into account that the multilayer thickness is in the nanometer range. The occurrence of virtually Al-free SiO_2 sublayers in all samples indicates that no atomic mixing took place during deposition.

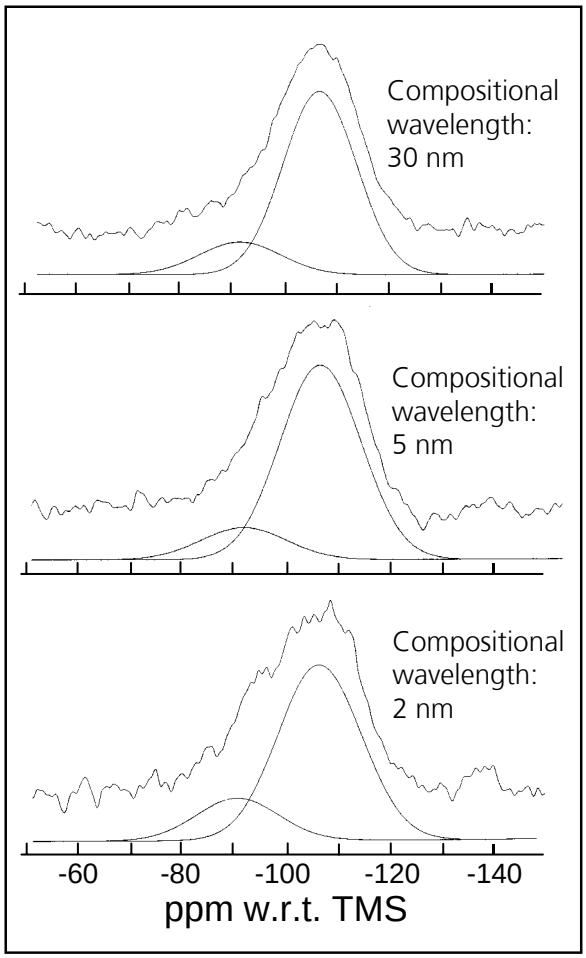

*Fig. 30: ^{29}Si NMR spectra of physical vapour deposited alumino silicate double layers with nominal thicknesses 30nm, 5 nm, and 2 nm, respectively. The three spectra are very similar, showing a main resonance at 110 ppm and a shoulder centered at ≈90 ppm (from **Schmücker et al., 2001**).*

Calcination of the PVD aluminium silicate films at 1000 °C (Fig. 31) reveals that only transition alumina has formed in series 1 (≈30 nm SiO_2/Al_2O_3 layer thickness), transition alumina plus minor amounts of mullite appear in series 2 and 3 (9 and 5 nm layer thickness, respectively), and only mullite formation has been observed in samples of series 4 (≈2 nm layer thickness). Samples of series 1-3 form mullite by reaction of transition alumina with silica at temperatures above 1200 °C. While the crystallization behaviour of series 1 to 3 corresponds to that of diphasic (type II) mullite precursors, aluminium silicate films of series 4 behave like ultrahomogeneous (type I) mullite precursors. This is a surprising result since series 4 aluminium silicate films are also diphasic even though on a nanometer scale. Obviously, a critical degree of chemical homogeneity exists,

suggesting that demixing zones below 2 nm do not suppress direct mullite formation but demixing zones above ≈5 nm do.

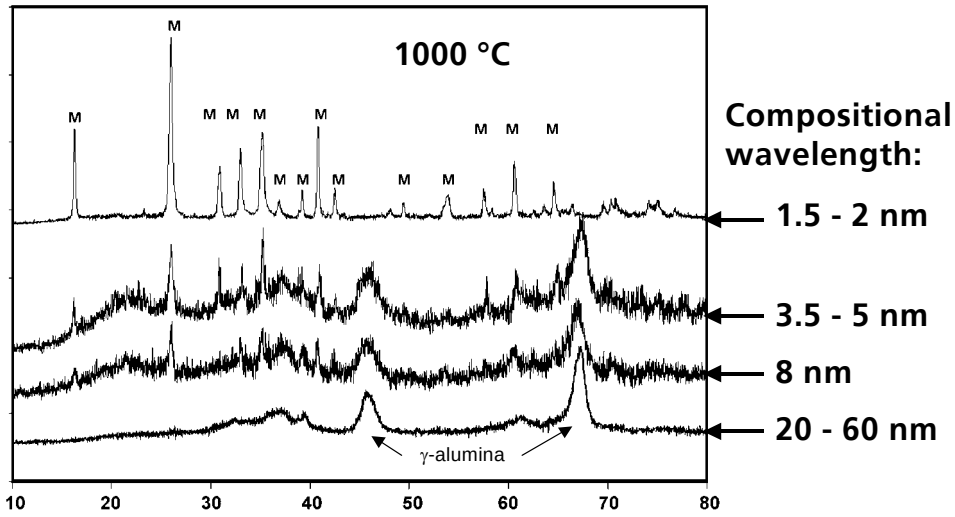

*Fig. 31: X-ray diffraction traces of physical vapor deposited alumino silicate double layers with different compositional wavelength after heat-treatment at 1000 °C. M=mullite; (from **Schmücker et al., 2001**).*

To explain the alteration in crystallization behaviour, it has been suggested that some interdiffusion-induced chemical homogenization occurs between adjacent Al_2O_3 and SiO_2 layers prior to crystallization, and that a certain homogenization volume is required for mullite nucleation (see Fig. 32).

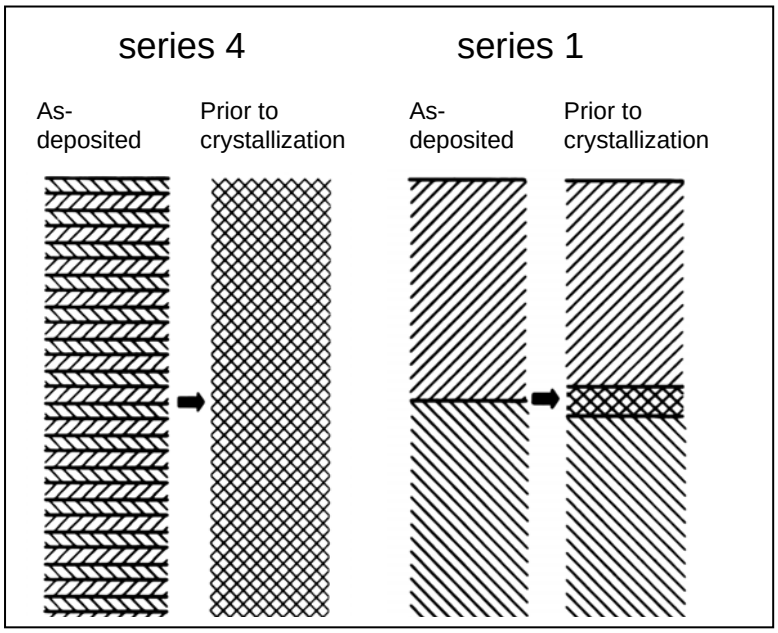

*Fig. 32: Schematic view of the interdiffusion-induced homogenization of Al_2O_3/SiO_2 double layers prior to mullitization, (from **Schmücker et al., 2001**).*

SiO_2,

Al_2O_3,

Al_2O_3 and SiO_2 mixed

If the zone of homogenization is 1-2 nm, then complete atomic mixing throughout the PVD film is achieved in series 4, since the SiO_2/Al_2O_3 layer thickness is of similar dimensions. According to this

scenario, both conditions, chemical mixing and the required volume for stable mullite nuclei are fulfilled and hence mullite formation at 1000 °C becomes possible. Relationships are completely different for instance in series 1, where the ultrathin zones of atomic mixing are separated by about 25 nm thick unmixed Al_2O_3 and SiO_2 layers. In that case the extension of the homogenized zones (≈1-2 nm) is believed to be below the critical size of a mullite nucleus, taking into account that stable growing mullite nuclei should be at least several unit cell dimensions in size.

The nature of type III gels

EB-PVD-derived diphasic aluminium silicate films consist of nanometer-sized segregation zones of Al_2O_3 and SiO_2, the latter proved by the typical 110 ppm signal in the ^{29}Si NMR spectrum. If the unmixing zones are sufficiently small (<2nm) direct mullite formation is not suppressed (see above). ^{29}Si NMR spectra of type III gels, on the other hand, do not indicate significant phase separation, but nonetheless spinel-type transition alumina instead of mullite forms as the first crystalline phase. Obviously, the different crystallization behaviour of type III and type I gels is beyond chemical or short-range order reasons.

To provide a clue to the different transformation behaviour, microstructures of type I and type III gels prepared either from TEOS plus Al-sec-butylate solutions (Voll, 1995) or TEOS plus $Al(NO_3)_3{\cdot}9H_2O$ solutions (Taake, 1999), respectively, were reexamined by transmission electron microscopy (**Schmücker, unpublished results**). Fig. 33 reveals significant morphological differences between type I and type III gels. Irrespective of the starting compounds, primary particles of 5-10 nm can be resolved in type III gels (Fig. 33 B, D). In contrast, only faint contours of nanometer-sized primary particles become visible in TEOS plus Al-sek-butylate derived type I gels (Fig. 33 A) which indicates intense particle aggregation. TEOS plus $Al(NO_3)_3{\cdot}9H_2O$ derived type I gels (Fig. 33 C), on the other hand, consist of agglomerated particles of 30-100 nm (see also Fig. 5). Complementary to the TEM investigations, TEOS plus $Al(NO_3)_3{\cdot}9H_2O$ derived gels were studied by small angle X-ray scattering (SAXS). Data analyses reveal particles sizes of 7 nm and 39 nm for type III and type I gels, respectively, (Okada, unpublished results) being in good accordance with microscopic data.

The microstructural analyses of type I and type III gels suggest that the crystallization behaviour is influenced by the particle sizes of the gels. Obviously, gels with intense aggregation of primary particles or with primary particles being several 10 nm in size tend to transform directly into mullite while particulate gels with primary particles below 10 nm form transition alumina as the first crystalline phase. This finding may be explained in terms of stable crystal nuclei sizes being assumed to be greater than ≈ 10 nm for mullite and smaller than 10 nm for γ-Al_2O_3.

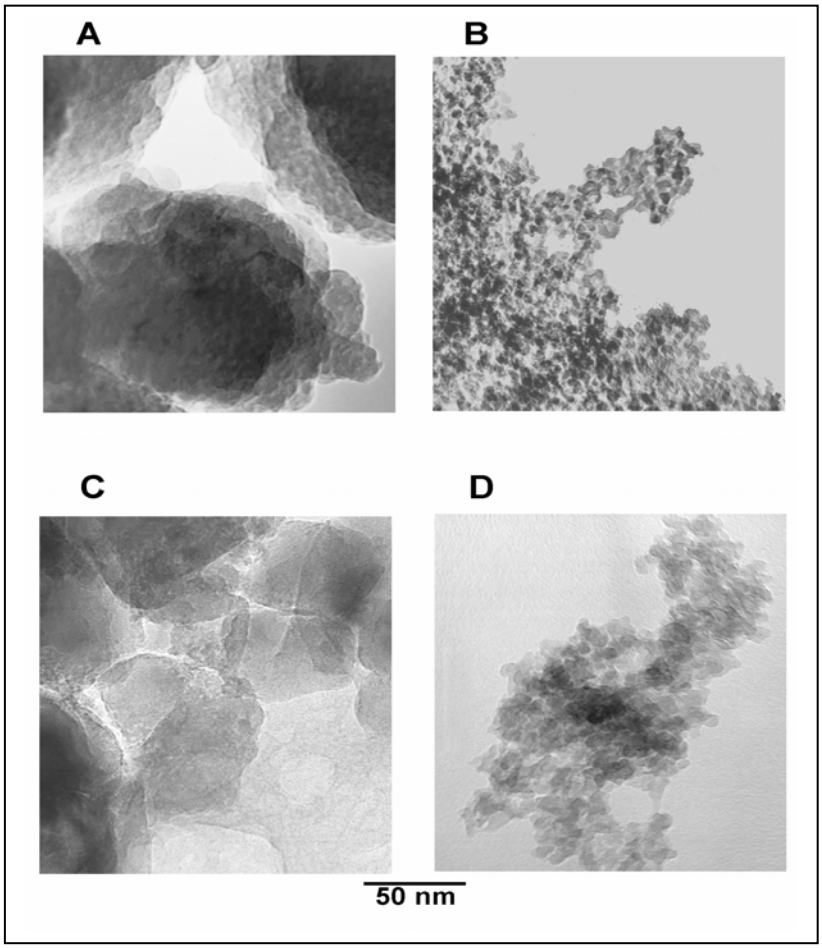

*Fig. 33: Microstructure of type I gels (a), (c), and of type III gels (b), (d). Starting materials were TEOS plus Al-sek-butylate solutions (a,b) and TEOS plus $Al(NO_3)_3 \cdot 9H_2O$ solutions (c,d). In contrast to type I gels, type III gels consist of primary particles smaller than 10 nm, (**Schmücker, unpublished**).*

Actually, there is experimental evidence from mullite crystal size data reported for early mullitization stages that stable mullite crystallites exceed 10 nm. Interestingly, crystallite sizes determined by various methods all range from ≈10 to ≈40 nm (Tab. 3). Transition alumina crystals, on the other hand, are well-known to be as small as 3 nm (e.g. Wefers, 1987). Thus, according to the present model, homogeneous aluminium silicate gels with particles greater than a stable mullite nucleus (≈ 10 nm) directly convert to mullite, while gels consisting of even smaller particles tend to form transition alumina crystals.

	Mullite crystal size [nm]	Method
Takamori and Roy (1973)	20	XRD
Tkalcec et al. (1998)	26-42	XRD
Takei et al. (1999)	≈ 15	FEG-SEM
Thom (2000)	25-40	XRD
Bartsch et al. (1999)	10-20	TEM
Johnson et al. (2001)	12.6	TEM
this paper, Fig. 10	≈ 20	TEM
this paper, Fig. 22	20-50	TEM

Table 3. Mullite crystallite size in early stage of crystallization

5. The origins of mullite crystallization

So far, the discourse on mullite precursors reveals that mullite generally originates from the non-crystalline state. High-density nucleation within the bulk of a non-crystalline aluminium silicate phase indicates a low energetic barrier to mullite nucleation, intuitively attributed to short range order similarities between mullite and its amorphous counterpart. In terms of classical nucleation theory it can be argued that high degrees of structural similarity reduce the surface energy (σ) of the nucleating phase but also the driving force of transformation (ΔG) is affected. However, the surface energy dominates the free enthalpy of transformation (σ^3 vs. ΔG^2)[§§], and hence a decrease of both thermodynamic parameters in total should lower the activation energy of nucleation. For mullite and non-crystalline aluminium silicates structural similarities refer to identical cation-oxgen polyhedra (SiO_4-tetrahedra, AlO_4-tetrahedra, AlO_6-octahedra, triclustered $(Si,Al)O_4$-tetrahedra) and similar polyhedral distribution.

Analogous correlations between the local structure of glass and crystal and nucleation behaviour were reported by several authors. Müller et al. (1993) reviewing literature data, stated that silicate glasses displaying "homogeneous" nucleation have short-range order similarities with their corresponding crystalline phase, in contrast to glasses typically transforming by heterogeneous nucleation events. The same was reported recently by Mastelaro et al. (2000) and Schneider et al. (2000b) investigating $Na_2Ca_2Si_3O_9$-, $CaSiO_3$-, $CaMgSi_2O_6$-, and $PbSiO_3$-glasses by means of EXAFS and ^{29}Si NMR spectroscopy.

Complete mullitization of ultrahomogeneous aluminium silicate phases (glasses, type I gels) at temperatures below 1000 °C is obviously the result of rapid nucleation and very short diffusion distances. It is noteworthy that a close structural relation between crystalline and non-crystalline material does not only affect mullite nucleation but also facilitates subsequent crystal growth considered as minor polyhedral rearrangement rather than diffusion over several nanometer distances. In contrast, diphasic mullite precursors display dissolution of alumina and subsequent diffusion in the siliceous phase prior to mullite nucleation. Depending on temperature, dissolution (below ≈1600 °C) or diffusion (above ≈1600 °C) is the rate-controlling step, thus leading to mullite formation either in the bulk of the siliceous melt or close to the SiO_2/Al_2O_3-interface (see ch. 3). Only minor Al_2O_3 supersaturation of the amorphous silicate is required to form mullite nuclei (Fig. 24) which again shows that the nucleation barrier must be low. Mullite crystal growth in diphasic starting materials, however, requires long-range diffusion of Al species throughout the silica-rich melt or, alternatively at high temperatures, Al-Si interdiffusion through the interfacial mullite layer.

The influence of SiO_2/Al_2O_3 segregation distance on mullitization temperature is depicted in Fig. 34. The data point 1 corresponds to aluminium silicate glasses or type I gels with compositional homogeneity on atomic level. The assumed "diffusional distance" is 0.2 nm. Data points 2-4 come

[§§] derived from classical nucleation theory where the activation energy of nucleation (E_{aN}) is given by $E_{aN} \propto \sigma^3 / T \Delta G^2$

from vapor deposited SiO_2-Al_2O_3 multilayers (see chapter 4) with layer thickness of 2, 5, and 30nm, respectively. Data points 5-7 refer to literature data obtained for diphasic gels (5), SiO_2 coated alumina particles (6) and alumina/silica powder admixtures (7). Data points 1 and 2 reveal that the transformation temperature of direct mullite forming precursors (type I) is not affected by original nanometer-sized segregation. This is consistent with the idea of compositional homogenization of the latter prior to crystallization (see ch. 4). In contrast, data for true diphasic materials (type II, data points 3-7) signal that mullite formation is shifted significantly toward higher temperatures if diffusional distances become greater.

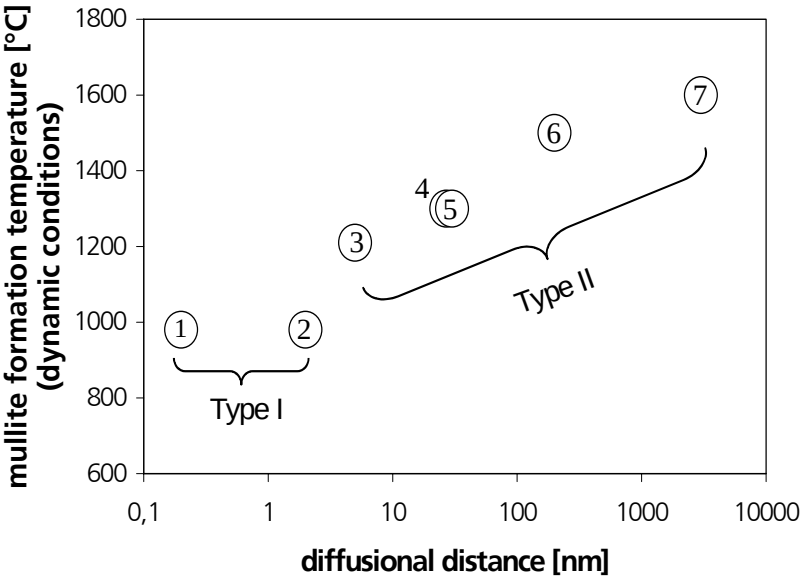

Fig. 34: SiO_2/Al_2O_3 segregation distance vs. mullitization temperature Data point 1 corresponds to aluminium silicate glasses or type I gels with compositonal homogeneity on atomic level. Data points 2-4 are from vapor deposited SiO_2-Al_2O_3 multilayers (see above) with layer thickness of 2, 5, and 30nm, respectively. Data points 5-7 refer to literature data obtained for diphasic gels (Wei and Halloran, 1988a,b), SiO_2 coated alumina particles (Wang and Sacks, 1996), and alumina/silica powder admixtures (Albers, 1994).

Obviously, the degree of SiO_2/Al_2O_3 segregation affects mullitization for the following reasons:

- *Dissolution of alumina*: small (highly curved) alumina particles display higher solubility in the siliceous phase than relatively coarse particles due to the Gibbs-Thompson effect; moreover, the solubility of metastable alumina phases is higher than that of α-Al_2O_3.
- *Critical nucleation concentration (CNC)*: The smaller the silica zones, the more rapid CNC is reached.
- *Growth of mullite crystals:* The diffusional distance of Al species throughout the silica-rich melt or Al-Si interdiffusion through the interfacial mullite layer, respectively, is directly controlled by the degree of SiO_2-Al_2O_3 segregation.

Mullite formation by topotactic reaction

So far, the discussion on the origin of mullite formation has emphasized that mullite typically nucleates within the bulk of a non-crystalline aluminium silicate phase. There are, however, exceptions to this rule, clearly demonstrating that mullite may form by a topotactic solid-state reaction if the crystalline parent phase is structurally related to mullite. Topotactic mullite formation has been reported for the conversion of polymorphic Al_2SiO_5 minerals sillimanite and andalusite (Guse et al., 1979, Pannhorst and Schneider, 1978) and, more recently, for the transformation of X-phase SiAlON (**Schmücker and Schneider, 1999b**).

Close structural similarities exist between sillimanite, andalusite and mullite (Fig. 35). Common structural features are AlO_6 chains running parallel to the respective crystallographic c-axes. The octahedral chains are crosslinked by SiO_4 and AlO_4 dimers (sillimanite), by $(Si,Al)O_4$ dimers and trimers (mullite), and by SiO_4 tetrahedra plus AlO_5 bipyramids (andalusite). Decomposition of sillimanite and andalusite leads to the formation of mullite crystals strictly oriented parallel to the parent phases accompanied by the exsolution of non-crystalline silica. The topotactic mullite formation suggests that the chains of AlO_6 octahedra are preserved during transformation and only the cross-linking cations and oxygen atoms have to undergo larger movements (Pannhorst and Schneider, 1978).

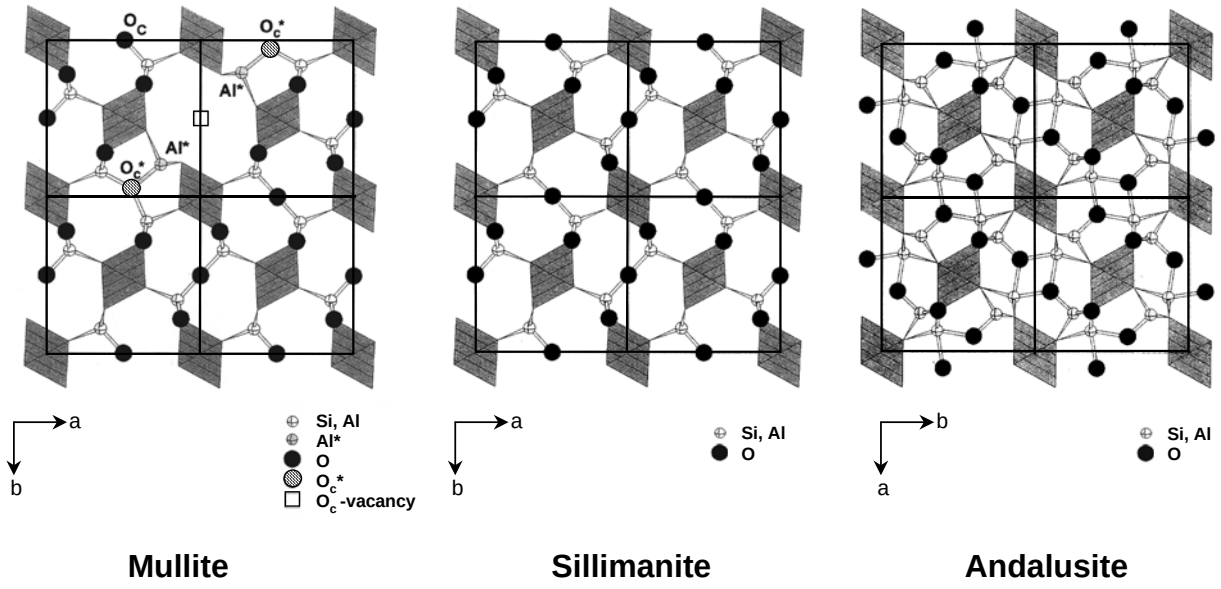

Fig. 35: Crystal structures of mullite (after Angel and Prewitt, 1986), sillimanite (Burnham, 1963), andalusite (Burnham and Buerger, 1961) all projected down their c-axes.

The andalusite-mullite conversion was recently reexamined by **Hülsmans et al. (2000a, b)**. In a comprehensive study the transformation behaviour of single crystal andalusite along the crystallographic a, b, and c axis was investigated by transmission electron microscopy. The

orientational relation c_{mul} || c_{and}, a_{mul} || b_{and}, b_{mul} || a_{and} was confirmed by electron diffraction and lattice imaging (Fig. 36). Moreover, it was found that mullite formation, in general, starts from the surfaces of the parent andalusite crystal. Growth of the mullite transformation zone, however, is highly anisotropic. Along [001], i.e. parallel to the octahedral chain direction, mullite crystals separated by tiny SiO_2 channels rapidly grow by a strictly topotactic reaction. In contrast, in directions perpendicular to [001], the transformation zone develops slowly by a dissolution/precipitation mechanism which includes the following steps:

- Dissolution of andalusite in the siliceous melt that has been formed during preceeding surface mullite formation.
- Diffusional transport of alumina from the andalusite core to the outer mullite zone throughout the siliceous melt.
- Slow growth of the outer mullite zone as long as the siliceous melt is Al_2O_3-supersaturated with respect to mullite.

Kinetic studies reveal that the topotactic transformation parallel [001] is about 10 times faster than the dissolution/precipitation controlled transformation along [100] and [010].

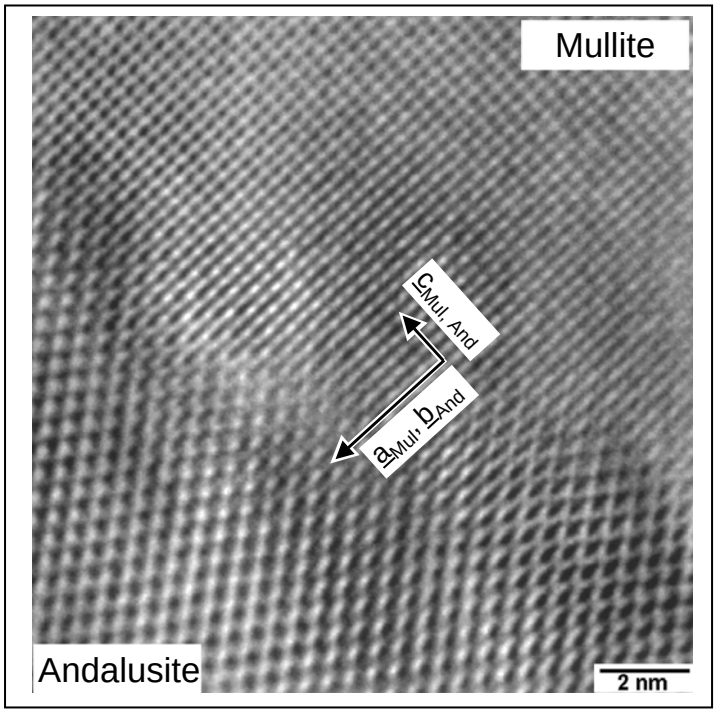

*Fig. 36 : High resolution TEM image of andalusite/mullite interface confirming topotactic transformation and the orientation relationship $c_{mullite}$ || $c_{andalusite}$ and $a_{mullite}$ || $b_{andalusite}$ (from **Hülsmans, 2000a**).*

Starting from the idea that topotactic transformation to mullite is controlled by the existence of AlO_6-octahedral chains occurring in the parent phase, **Schmücker and Schneider (1999b)** investigated the oxidation-induced transformation of X-phase sialon (Fig. 37). Although the structure of X-sialon is not fully understood, there are clear indications of structural relations to

mullite. It is suggested that X-sialon is built of AlO_6 chains running parallel to its triclinic b axis crosslinked by a complex tetrahedral network (Thompson and Korgul, 1983, Fig.38).

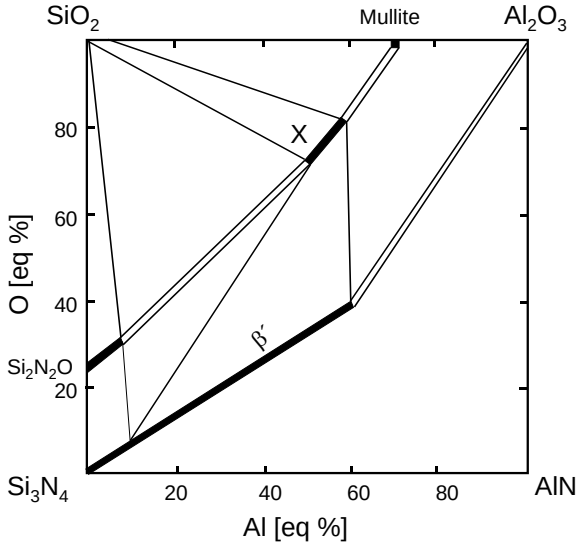

Fig. 37: Si_3N_4-Al_2O_3-AlN-SiO_2 subsolidus phase diagram (from Zhou et al., 1995)

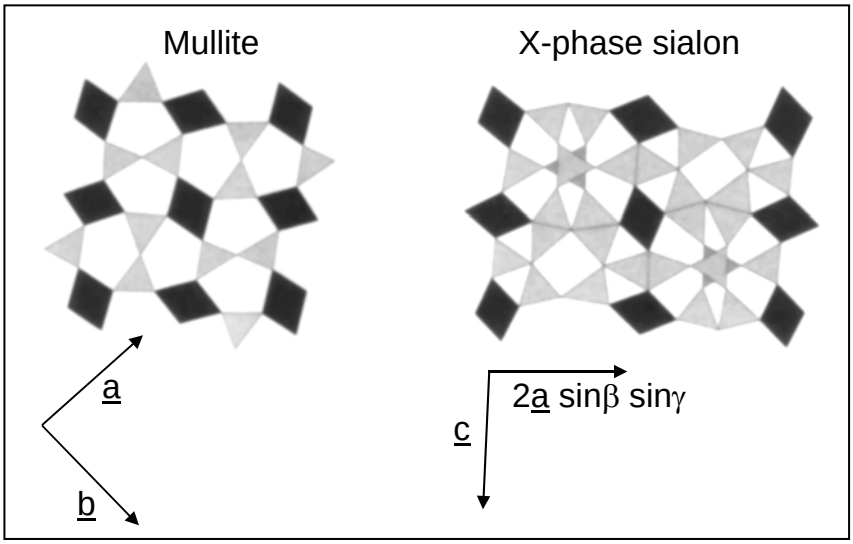

Fig. 38: Structural similarities between mullite (simplified average structure) and X-phase sialon become obvious when projected perpendicular to their respective directions of octahedral chains. Octahedral chains run parallel to c-axis in mullite and parallel to b-axis in X-phase sialon (after Thompson and Korgul, 1983).

The X-phase-mullite transformation was studied by TEM using polycrystalline X-sialon ceramics with typical grain sizes of 1-3 µm fired at 1250 °C in air (1h) to induce superficial mullite formation by oxidation. TEM investigations on partially oxidized X-sialon revealed the formation of sub-micron sized mullite crystals embedded in a glassy matrix. Obviously all newly formed mullite crystallites occurring in a former X-phase sialon grain are orientated in the same way (Fig. 39) which is a first indication of topotactic transformation. Analysis of the electron diffraction patterns within the transformation region (Fig. 39) reveals that (110) mullite lattice planes (d=5.38 Å) are parallel to (100) of the adjacent X-phase sialon (d=7.86 Å). The obtained diffraction patterns correspond to the $[1\ \bar{1}\ 4]_{Mullite}$ and $[0\ \bar{3}\ \bar{2}]_{X\text{-}phase}$ zone axes, respectively.

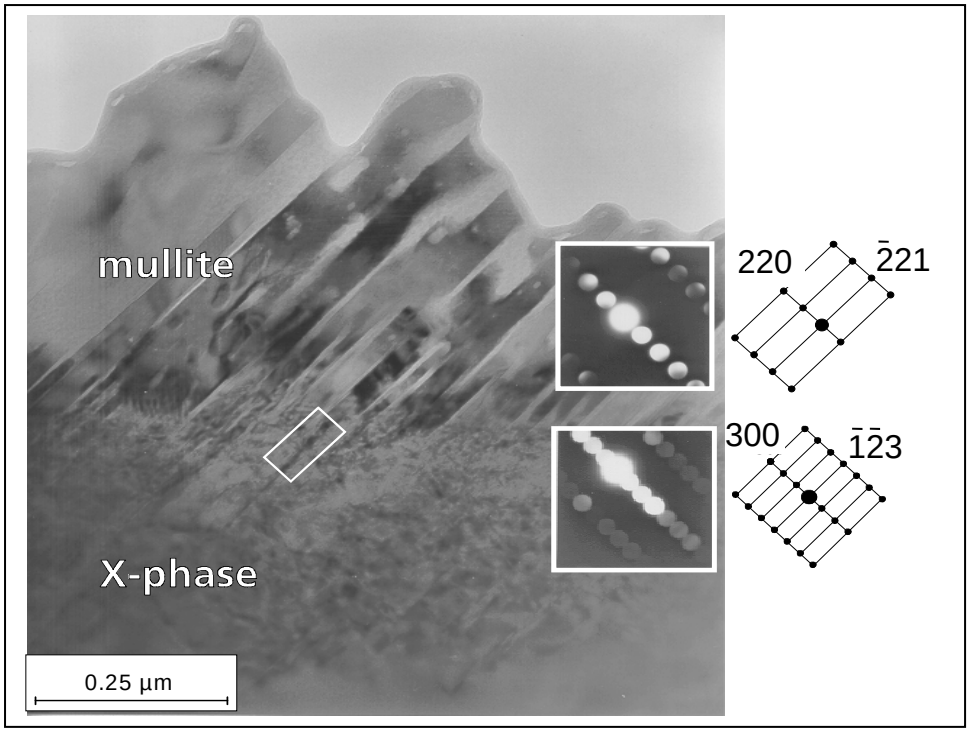

*Fig. 39: TEM photograph of an X-phase sialon grain partially transformed into mullite (1250 °C, 1h). Electron diffraction patterns (CBED) show parallel lattice planes of X-phase sialon and mullite; all mullite crystallites are oriented in the same way (**Schmücker and Schneider, 1999b**).*

Parallel lattice planes of $(1\ 1\ 0)_{Mullite}$ and $(1\ 0\ 0)_{X\text{-}phase}$ are also identified in high resolution transmission electron microscopic images of interfacial areas (Fig. 40) and it becomes obvious that two $(1\ 0\ 0)_{X\text{-}phase}$ lattice planes match three $(1\ 1\ 0)_{Mullite}$ lattice planes. Moreover, the lattice fringe images show that there exists a structural transition range between X-phase sialon and mullite rather than a sharp interface.

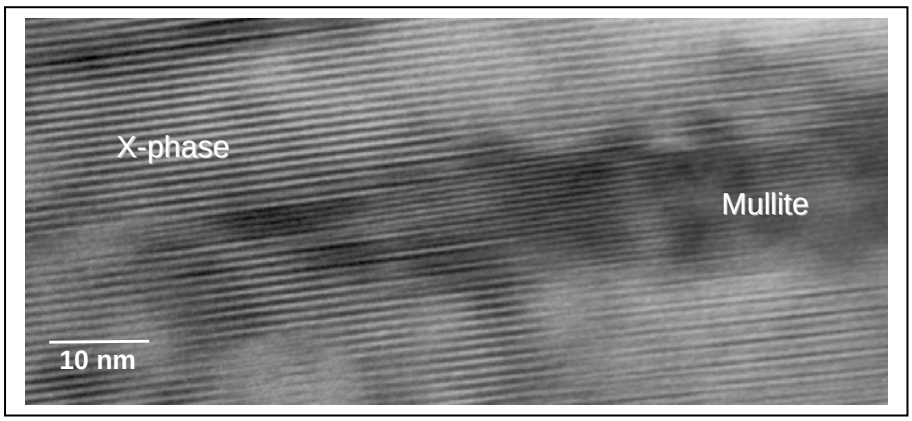

*Fig. 40: Detail of Fig. 39 (white box): Parallel lattice planes of mullite (1 1 0) and of X-phase sialon (1 0 0) become visible in the high-resolution micrograph (**Schmücker and Schneider, 1999b**).*

As it was suggested that topotactic X-sialon-mullite transformation is controlled by chains of AlO_6 octahedra acting as common features of both structures, the orientational relationship

$b_{X\text{-phase}} \parallel c_{mullite}$ was expected. Actually, the electron diffraction patterns of Fig. 39 are consistent with that idea, since $(1\ 0\ 0)_X$ which contains $[0\ 1\ 0]_X$ is orientated parallel to $(1\ 1\ 0)_{Mu}$ which contains $[0\ 0\ 1]_{Mu}$. Moreover, the angles between the respective zone axes and the corresponding octahedral chain directions, i.e. $[0\ 1\ 0]_X$ / $[0\ {-3}\ {-2}]_X$ and $[0\ 0\ 1]_{Mu}$ / $[1\ {-1}\ 4]_{Mu}$ are virtually the same (137.0 and 138.8°, respectively). Thus, the orientational relation between X-phase sialon and mullite suggested in Fig. 36 is established. The topotactic X-phase-mullite conversion, therefore, is a further indication of the transformation-controlling role of AlO_6 octahedral chains irrespective of the linking structural elements.

References

I. A. Aksay, D. M. Dabbs, M. Sarikaya, Mullite for structural, electronic, and optical applications, J. Amer. Ceram. Soc. 74 (1991) 2343-58

I. A. Aksay, J. A. Pask, Stable and metastable equilibria in the system SiO_2-Al_2O_3, J. Am. Ceram. Soc. 58 (1975) 507-12

W. Albers, Ph. D. Thesis, Univ. Hannover, 1994

R.J. Angel, C.T. Prewitt, Crystal structure of mullite: a re-examination of the average structure. Amer. Min. 71 (1986) 1476-1482.

T. Ban, S. Hayashi, A. Yasumori, K. Okada, Calculation of metastable immiscibility region in the Al_2O_3-SiO_2 system, J. Mater. Res. 11 (1996) 1421-27

M. Bartsch, B. Saruhan, **M. Schmücker**, H. Schneider, Novel low-temperature processing route of dense mullite ceramics by reaction sintering of amorphous SiO_2 coated γ-Al_2O_3 particle nanocomposites. J. Amer. Ceram. Soc. 82 (1999) 1388-92

A.R. Boccaccini, T.K. Khalil, M. Bücker, Activation energy for the mullitization of a diphasic gel obtained from fumed silica and boehmite sol, Mat. Lett. 38 (1999) 116-20

P.R. Bodart, J. Parmentier, R.K. Harris, D.P. Thompson, Aluminium environments in mullite and an amorphous sol-gel precursor examined by ^{27}Al triple quantum MAS NMR, J. Phys. Chem. Solids 60 (1999) 223-28

I.W.M. Brown, K.J.D. MacKenzie, M.E. Bowen, R. H. Meinhold, Outstanding problems in the kaolinite-mullite reaction sequence investigated by ^{29}Si and ^{27}Al solid-state nuclear magnetic resonance: II. High-temperature transformations of metakaolinite. J. Am. Ceram. Soc. 68 (1985) 298-301

C.W. Burnham, M. J. Buerger, Refinement of the crystal structure of andalusite, Z. Krist. 115 (1961) 269-90

C. W. Burnham, Refinement of the crystal structure of sillimanite, Z. Krist. 118 (1963) 127-48

A. K. Chakraborty, D.K. Ghosh, Reexamination of kaolinite –to-mullite reaction series, J. Amer. Ceram. Soc. 61 (1978) 170-73

K. K. Chawla, H. Schneider, **M. Schmücker**, Z.R. Xu, Oxide fiber/oxide matrix composites, in: Processing and design issues in high temperature materials (eds. N. S. Stoloff, R. H. Jones), The Minerals, Metals & Materials Society, Warrendale PA, 1997, 235-245

Ph. Colomban, Structure of oxide gels and glasses by infrared and Raman scattering, J. Mater. Sci. 24 (1989) 3011-20

P. C. Dokko, J. A. Pask, K.S. Mazdiyasni, High temperature mechanical properties of mullite under compression, J. Am. Ceram. Soc. 60 (1977) 150-55

G. Engelhardt and D. Michel, "High Resolution Solid State NMR of Silicates and Zeolithes" John Wiley and Sons, New York, 1987

R.X. Fischer, H. Schneider, **M. Schmücker**, Crystal structure of Al-rich mullite, Amer. Min. 79 (1994) 983-990

M. Fukuoka, Y. Onoda, S. Inoue, K. Wada, A. Nukui, A. Makashima J. The role of precursors in the structure of SiO_2-Al_2O_3 sols and gels by the sol-gel-process, Sol-Gel Sci. Tech. 1 (1993) 47-53

M.S.J. Gani, R. McPherson, Crystalization of mullite from Al_2O_3-SiO_2 glasses, J. Austr. Ceram. Soc. 13 (1977a) 21-24

M.S.J. Gani, R. McPherson, Glass formation and phase transformation in plasma prepared Al_2O_3-SiO_2 powders, J. Mater. Sci. 12 (1977b) 999-1009

R. L. Gentilman, Current and emerging materials for 3-5 micron IR transmission, Infrared Opt. Transm. Mater. Proc. SPIE 683 (1986) 2-11

C. Gerardin, S. Sundaresan, J. Bernziger, A. Navrotsky, Structural investigation and energetics of mullite formation from sol-gel-precursors, Chem. Mater. 6 (1994) 160-168

W. Guse, H. Saalfeld, J. Tjandra, Thermal transformation of sillimanite single crystals, N. Jb. Miner. Mh. (1979) 175-185

T. Heinrich and F. Raether, Structural characterization and phase development of sol-gel derived mullite and its precursors, J. Non-Cryst. Solids 147 &148 (1992) 152-56

B. Hildmann, H. Schneider, **M. Schmücker**, High temperature behaviour of polycrystalline Alumo-sillcate fibers with mullite bulk composition: II. Kinetics of γ-Al_2O_3 -mullite transformation J. Europ. Ceram. Soc., 16 (1996) 287-92

Y. Hirata, S. Matsushita, Y. Ishihara, H. Katsuki, Colloidal processing and mechanical properties of whisker-reinforced mullite matrix composites, J. Am. Ceram. Soc. 74 (1991) 2438-42

D.W. Hoffman, R. Roy, S.Komarneni, Diphasic xerogels, a new class of materials: phases in the system Al_2O_3-SiO_2, J. Am. Ceram. Soc. 67 (1984) 468-71

J. C. Huling, L. Messing, Epitactic nucleation of spinel in aluminium silicate gels and effect on mullite crystallization, J. Am. Ceram. Soc. 74 (1991) 2374-81

J. C. Huling, L. Messing, Chemistry-crystallization relations in molecular mullite gels, J. Non-Cryst. Solids 147&148 (1992) 213-21

A. Hülsmans, **M. Schmücker**, W. Mader, H. Schneider, The transformation of andalusite to mullite and silica, Part I: Transformation mechanism in $[001]_A$ direction, Am. Min. 85 (2000a) 980-986

A. Hülsmans, **M. Schmücker**, W. Mader, H. Schneider, The transformation of andalusite to mullite and silica, Part II: Transformation mechanism in $[100]_A$ and $[010]_A$ direction, Am. Min. 85 (2000b) 987-992

M.J. Hyatt, N. P. Bansal, Phase transformations in xerogels of mullite composition, J. Mater. Sci. 25 (1990) 2815-21

M. Iwata, K. Oshima, T. Isoda, M. Arai, K. Nakano, A. Kamiya, Mechanical properties and microstructures of fiber-reinforced silicon nitride and mullite composites. In: Abstracts of the anual meeting of the ceramic society of Japan, Paper #2E36, Ceramic Society of Japan, Tokyo, 1989

P.F. James, Y. Iqbal, U.S. Jais, S. Jordery, W.E. Lee, Crystallization of silicate and phosphate glasses, J. Non-cryst. Solids, 219 (1997) 17-29

I. Jaymes and A. Douy, New aqueous mullite precursor synthesis. Structural study by ^{27}Al and ^{29}Si NMR spectroscopy, J. Europ. Ceram. Soc. 16 (1996) 155-60

B. R. Johnson, W.M. Kriven, J. Schneider, Crystal structure development during devitrification of quenched mullite, J. Europ. Ceram. Soc. 21 (2001) 2541-62

S. Kanzaki, H. Tabata, T. Kumazawa, S. Ohta, Sintering and mechanical properties of mullite, J. Amer. Ceram. Soc., 68 (1985) c6-c7

S. Kanzaki, M. Ohashi, H. Tabata, T. Kurihara, S. Iwai, S. Wakabayashi, Mullite-silica ceramics for insulating substrate material, Ceramic Trans. Vol.6, 389-400, Am. Ceram. Soc. Westerville OH, 1990

H.J. Kleebe, F. Siegelin, T. Straubinger, G. Ziegler, Conversion of Al_2O_3-SiO_2 powder mixtures to 3:2 mullite following the stable or metastable phase diagram, J. Europ. Ceram. Soc. 21 (2001) 2521-33

F. J. Klug, S. Prochazka, R. H. Doremus, Alumina-silica phase diagram in the mullite region, J. Am. Ceram. Soc. 70 (1987) 750-59

S. Komarneni, R. Roy, Application of compositionally diphasic xerogels for enhanced densification, the system Al_2O_3-SiO_2. J. Am. Ceram. Soc. 69 (1986) c155-56

T. Koyama, S. Hayashi, A. Yasumori, K. Okada, **M. Schmücker**, H. Schneider, Microstructure and mechanical properties of mullite/zirconia composites prepared from alumina and zircon under various firing conditions, J. Europ.Ceram. Soc. 16 (1996) 231-37

E. D. Lacy, Aluminium in glasses and melts, Phys. Chem. Glasses 4 (1963) 234-238

D. X. Li and W. J. Thomson, Mullite formation kinetics of a single phase gel, J. Amer. Ceram. Soc. 73 (1990) 964-69

D. X. Li and W. J. Thomson, Mullite formation from non-stoichiometric diphsic precursors, J. Amer. Ceram. Soc. 74 (1991) 2382-87

I. M. Low, R. McPherson, The origins of mullite formation, J. Mater. Sci. 24 (1989) 926-36

J. F. MacDowell, G. H. Beall, Immiscibility and crystallization in Al_2O_3-SiO_2 glasses, J. Amer. Ceram. Soc. 52 (1969) 17-25

M. Mägi, E. Lipmaa, A. Samoson, G. Engelhardt, A. R. Grimmer, Solid state high resolution silicon-29 chemical shifts in silicates, J. Phys. Chem. 88 (1984) 1518-1522

K. J. D. Mackenzie, R. H. Meinhold, J. E. Patterson, H. Schneider, **M. Schmücker**, D. Voll, Structural evolution in gel-derived mullite precursors, J. Europ. Ceram. Soc. 16 (1996) 1299-1308

V. R. Mastelaro, E. D. Zanotto, N. Lequeux, R. Cortès, Relationship between short-range order and ease of nucleation in $Na_2Ca_2Si_3O_9$, $CaSiO_3$ and $PbSiO_3$ glasses, J. Non-Cryst.Solids 262 (2000) 191-199

J. McManus, S.E. Ashbrook, K.J.D. MacKenzie, S. Wimperis, ^{27}Al multiple quantum MAS and ^{27}Al {^{1}H} CPMAS NMR study of amorphous aluminosilicates, J. Non-Cryst. Solids 282 (2001) 278-290

R. H. Meinhold, R. C. T. Slade, T. W. Davies, High field ^{27}Al MAS NMR studies of the formation of metakaolinite by flash calcination of caolinite, Appl. Magn. Reson. 4 (1993) 141-155

L. H. Merwin, A. Sebald, H. Rager, H. Schneider, ^{29}Si and ^{27}MAS NMR spectroscopy of mullite. Phys. Chem. Minerals, 18 (1991) 47-52

H. Morikawa, S. Miwa, M. Miyake, F. Marumo, T. Sata, Structural analysis of SiO2-Al2O3 glasses, J. Amer. Ceram. Soc. 65 (1982) 78-81

E. Müller, K. Heide, E.D. Zanotto, Molecular structure and nucleation in silicate glasses, J. Non-cryst. Solids 155 (1993) 56-66

S. Musikant, Development of a new family of improved infrared dome ceramics, Emerging. Opt. Mater. Proc. SPIE, 297 (1981) 2-12

K. Okada and N. Otsuka, Characterization of the spinel phase from SiO_2-Al_2O_3 xerogels and the formation process of mullite, J. Amer. Ceram. Soc. 69 (1986) 652-56

K. Okada and N. Otsuka, Preparation of transparent mullite films by dip-coating method, Ceram. Trans. Vol. 6, 425-30, Am. Ceram. Soc. Westerville OH, 1990

K.Okada, N. Otsuka, S. Somiya, Review of mullite synthesis routes in Japan, Am. Ceram. Soc. Bull. 70 (1991) 1633-39

K. Okada, C. Aoki, T. Ban, S. Hayashi, A. Yasumori, Effect of Aging Temperature on the Structure of Mullite Precursor Prepared from Tetraethoxysilane and Aluminum Nitrate in Ethanol Solution, J. Europ. Ceram. Soc. 16 (1996) 149-153

M. Okuno, Y. Shimada, **M. Schmücker**, H. Schneider, W. Hoffbauer, M. Jansen, LAXS and Al-NMR studies on the temperature induced changes of non-crystalline single phase mullite precursors J. Non-Cryst. Solids 210 (1997) 41-47

J. Ossaka, Tetragonal mullite like phase from co-precipitated gels, Nature 191 (1961) 1000-01

Pannhorst, W.; Schneider, H.: The high temperature transformation of andalusite (Al_2Si0_5) into 3/2-mullite ($3Al_20_32Si0_2$) and vitreous silica ($Si0_2$). Min. Mag. 42 (1978)195-198

M.P.J. Peeters, A.P.M. Kentgens, A ^{27}Al MAS, MQMAS and off-resonance nutation NMR study of aluminium containing silica-based sol-gel materials, Solid State NMR, 9 (1997) 203-217

J. C. Pouxviel, J. P. Boilot, A. Lecomte, A. Dauger, Growth process and structure of aluminosilicate gels, J. Phys. 48 (1987) 921-925

J. C. Pouxviel, J. P. Boilot, Gels from a double alkoxide $(BuO)_2$-Al-O-Si-$(OEt)_3$, J. Mater. Sci. 24 (1989) 321-27

S. H. Risbud, J. A. Pask, Calculated thermodynamic data and metastable immiscibility in the system SiO_2-Al_2O_3, J. Amer. Ceram. Soc. 60 (1977) 419-424

S. H. Risbud, R. J. Kirkpatrick, A. P. Taglialavore, B. Montez, Solid state NMR evidence of 4-, 5-, and 6-fold aluminium sites in roller-quenched SiO_2-Al_2O_3 glasses, J. Amer. Ceram. Soc. 70 (1987) c10-12

M. D. Sacks, N. Bozkurt, G.W. Scheiffele, Fabriction of mullite and mullite matrix composites by transient viscous sintering of composite powders, J. Am. Ceram. Soc. 74 (1991) 2828-37

H. Saalfeld, W. Guse, Structure refinement of 3:2-mullite, N. Jb. Miner. Abh. 13 (1981) 145-50

M. Schmücker, W. Albers, H. Schneider, Mullite formation by reaction sintering of quartz and α-alumina - a TEM study, J. Europ. Ceram. Soc.14 (1994) 511-515

M. Schmücker, H. Schneider, M. Poorteman, F. Cambier, R. Meinhold, Formatlon of Al_2O_3-rich glasses in the System SiO_2-Al_2O_3, J. Europ. Ceram Soc.15 (1995) 1201-05

M. Schmücker, H. Schneider, A new approach on the coordination of Al in non-crystalline gels and glasses of the system SiO_2-Al_2O_3, Ber. Bunsenges. Phys. Chem. 100 (1996) 1550-1553

M. Schmücker, K.J.D. Mackenzie, H. Schneider, R. Meinhold, NMR-studies on rapidly solidified SiO_2-Al_2O_3 -and SiO_2-Al_2O_3-Na_2O glasses, J. Non-Cryst. Solids 217 (1997) 99-105

M. Schmücker, H. Schneider, Sonnenofenunterstützte Forschungsarbeiten im System SiO_2 - Al_2O_3, in : Solare Chemie und Materialforschung, M. Becker, K.-H. Funken (Hrsg.) C. F. Müller Verlag, Heidelberg, 1997, 125-33

M. Schmücker, H. Schneider, K.J.D Mackenzie, Mechanical amorphization of mullite and recrystallization. J. non-cryst. Solids 226 (1998) 99-103

M. Schmücker, H. Schneider, K.J.D. Mackenzie, M. Okuno, Comparative Al NMR and LAXS studies on Rapidly Quenched Aluminosilicate glasses J. Europ. Ceram. Soc. 19 (1999) 99-103

M. Schmücker, H. Schneider, Structural development of single phase mullite gels, J. Sol-Gel Sci. Tech. 15 (1999a) 191-199

M. Schmücker, H. Schneider, Transformation of X-phase Sialon into mullite, J. Amer. Ceram. Soc. 82 (1999b) 1934-37

M. Schmücker, W. Hoffbauer, H. Schneider, Constitution and Crystallization Behaviour of Ultrathin Physical Vapor Deposited (PVD) Al_2O_3/SiO_2 Laminates, J. Europ. Ceram. Soc., 21 (2001) 2503-07

M. Schmücker, H. Schneider, New evidence for tetrahedral triclusters in alumino silicate glasses, J. non-cryst. Solids, in press (2002a)

M. Schmücker, B. Hildmann, H. Schneider, The mechanisms of 2/1- to 3/2-mullite transformation, Amer. Min. 87 (2002b) 1190-93

H. Schneider, E. Eberhard, Thermal expansion of mullite, J. Am. Ceram. Soc. 73 (1990) 2073-76

H. Schneider, L. Merwin, A. Sebald, Mullite formation from non-crystalline precursors, J. Mater. Sci. 27 (1992) 805-12

H. Schneider, **M. Schmücker**, K. Ikeda, W.A. Kaysser, Optically translucent mullite ceramics. J. Am. Ceram. Soc. 76 (1993a) 2912-16

Schneider, H., Saruhan, B., Voll, D., Merwin, L., Sebald, A.: Mullite precursor phases. J. Europ. Ceram. Soc., 11 (1993b) 87-94

H. Schneider, K. Okada, J. A. Pask, "Mullite and mullite ceramics", John Wiley & Sons, Chichester (1994a)

H. Schneider, D. Voll, B. Saruhan, J. Sanz, G. Schrader, C. Rüscher, A. Mosset, Synthesis and structural characterization of non-crystalline mullite precursors, J. Non-Cryst. Solids 17 (1994b) 262-271

H. Schneider, D. Voll, B. Saruhan, **M. Schmücker**, T. Schaller, A. Sebald, Constitution of the γ-alumina phase in chemically produced mullite precursors, J. Europ. Ceram. Soc. 13 (1994c) 441-48

H. Schneider, **M. Schmücker**, J. Göring, B. Kanka, J. She, P. Mechnich, Porous alumino silicate fiber/mullite matrix composites: fabrication and properties, Ceram. Trans Vol.115, 415-434, Amer. Ceram. Soc, Westerville, OH, 2000a

J. Schneider, V. R. Mastelaro, H. Panepucci and E. D. Zanotto, ^{29}Si MAS–NMR studies of Q^n structural units in metasilicate glasses and their nucleating ability, J. Non-Cryst. Solids, 273 (2000b) 8-18

K. Srikrishna, G. Thomas, R. Martinez, M. P. Corral, S. De Aza, J. S. Moya, Kaolinite-mullite reaction series: A TEM study, J. Mater. Sci. 25 (1990) 607-12

S. Sundaresan, I. A. Aksay, Mullitization of diphasic aluminosilicate gels, J. Am. Ceram. Soc. 74 (1991) 2388-92

C. Taake, Ph.D. thesis, University of Hannover, 1999

T. Takamori, R. Roy, Rapid crystallization of SiO_2-Al_2O_3 glasses, J. Amer. Ceram. Soc. 56 (1973) 639-644

T. Takei, Y. Kameshima, A. Yasumori, K. Okada, Crystallization kinetics of mullite in alumina-silica fibers, J. Amer. Ceram. Soc. 82 (1999) 2876-80

T. Takei, Y. Kameshima, A. Yasumori, K. Okada, Calculation of metastable immiscibility region in the Al_2O_3- SiO_2 system using molecular dynamics simulation, J. Mater. Sci. 15 (2000) 186-93

T. Takei, Y. Kameshima, A. Yasumori, K. Okada, Crystallization kinetics of mulite from Al_2O_3-SiO_2 glasses under non-isothermal conditions, J. Europ. Ceram. Soc. 21 (2001) 2487-93

A.Taylor, D. Holland, The chemical synthesis and reaction sequence of mullite, J. Non-Cryst. Solids 152 (1993) 1-7

M. Thom, Diploma thesis, University of Köln, 2000

D. P. Thompson, P. Korgul, "Sialon X-Phase", in: *F.L. Riley (ed.)"Progress in Nitrogen Ceramics"*, Martinus Nijhoff Publishers, Boston, 1983, 375-80

E. Tkalcec, R. Nass, J. Schmauch, H. Schmidt, S. Kurajica, A. Bezjak, H. Ivankovic, Crystallization kinetics of mullite from single phase gel determined by isothermal differential scanning calorimetry, J. Non-cryst. Solids 223 (1998) 57-72

D. Voll, Ph. D. Thesis, University of Hannover (1995)

D. Voll, A. Beran, H. Schneider, Temperature-dependent dehydration of sol-gel-derived mullite precursors: An FTIR spectroscopy study, J. Europ. Ceram. Soc. 18 (1998) 1101-1106

K. Wang, M. Sacks, "Mullite formation by endothermic reaction of α-Al_2O_3/silica microcomposite particles, J. Amer. Ceram. Soc. 79 (1996) 12-16

K. Wefers, C. Misra, Oxides and hydroxides of aluminium, Alcoa Technical Paper No. 19, Revised, Alcoa Lab, Pittsburgh PA, 1987

W.-Ch. Wei, J. W. Halloran, Phase transformation of diphasic aluminosilicate gels, J. Am. Ceram. Soc. 71 (1988a) 166-72

W.-Ch. Wei, J. W. Halloran, Transformation kinetics of diphasic aluminosilicate gels, J. Am. Ceram. Soc. 71 (1988b) 581-87

B. E. Yoldas, Mullite formation from aluminium and silicon alkoxides, Ceram. Trans. 6 (1990) 255-63

B. E. Yoldas, D. E. Partlow, Formation of mullite and other alumina-based ceramics via hydrolytic polycondensation of alkoxides and resultant ultra- and microstructural effects, J. Mater. Sci. 23 (1988) 1895-1900

Y. Zhou, J. Fleugels,T. Laoui, P. Ratchev, O. van der Biest, Preparation and properties of X-sialon, J. mater. Sci. 30 (1995) 4584-90